Numerical investigation of external sulfate attack and its effect on chloride binding and diffusion in concrete

Zhang, Cheng-lin; Chen, Wei-kang ; Mu, Song ; Šavija, Branko; Liu, Qing-feng

DOI
10.1016/j.conbuildmat.2021.122806

Publication date
2021

Document Version
Accepted author manuscript

Published in
Construction and Building Materials

Numerical investigation of external sulfate attack and its effect on chloride binding and diffusion in concrete

Cheng-lin Zhang[a], Wei-kang Chen[a], Song Mu[c], Branko Šavija[d] and Qing-feng Liu[a,b*]

a- State Key Laboratory of Ocean Engineering, School of Naval Architecture, Ocean & Civil Engineering, Shanghai Jiao Tong University, Shanghai, China;

b- Collaborative Innovation Center for Advanced Ship and Deep-Sea Exploration (CISSE), Shanghai, China

c- State Key Laboratory of High Performance Civil Engineering Materials, Jiangsu Research Institute of Building Science, Nanjing, China

d- Delft University of Technology, Stevinweg 1, 2628 CN Delft, The Netherlands

Abstract

Reinforced concrete (RC) structures may suffer from serious durability problems during long-term service. To investigate the deterioration of RC structures subjected to the dual attacks of chlorides and sulfates, this study proposes a coupled model for external sulfate attack (ESA) and its effect on chloride binding and diffusion. To account for the influence of sulfate attack on chloride binding, a reduction function is proposed. The effect of sulfate-induced damage on the chloride diffusion and chloride binding is considered through a damage function. The coupled model is calibrated against third-party experimental data from multiple perspectives. Some important factors such as solution concentration, immersion time, curing time and water-cement ratio, as well as how these factors affect the impact of sulfate attack on chloride transport, were elaborated. The findings may bring insights to the durability design of RC structures serving in harsh environments.

Keywords: External sulfate attack; Damage evolution; Binding capacity; Chloride diffusivity; Multi-phase

---

*) *Corresponding author:*

Email: liuqf@sjtu.edu.cn (Q.-F. Liu)

1. Introduction

Deterioration of reinforced concrete (RC) structures is often caused by external sulfate attack (ESA) and chloride-induced rebar corrosion during the long-term service period. The ESA is widely recognized to degrade concrete matrix and corrode rebars through a series of physicochemical reactions [1–4]. When penetrating into concrete interior, sulfate ions react with cement hydration products, leading to the formation of ettringite and/or gypsum, which initially reduces the porosity but may later cause the microcracking and damage of the concrete matrix [5–7]. During the process of sulfate ingress, active rebar corrosion would be induced by the transform from the protective passive iron oxide film to a less protective sulfate one [8,9].

As a trigger for the initiation of rebar corrosion, chloride penetration is also a major concern to the durability of RC structures [10–13], especially when the concrete is damaged [14-16]. A portion of chloride ions, once in concrete, react with cement hydration products, while some are adsorbed on the hydration products. The former process is called chemical chloride binding, while the latter is termed physical chloride adsorption. In total, they are referred to as the chloride binding effect [17–20]. The remaining chloride ions in the pore solution, namely free chloride ions, would diffuse internally and gradually accumulate around steel rebars. When the chloride content at the rebar level exceeds a certain value, active corrosion may start [21]. It is well known that it is only the free chloride ions that are responsible for rebar corrosion. As a consequence, factors that influence the chloride binding are directly related to the risk of rebar corrosion [20,22–28].

Sulfate and chloride ions coexist around the RC structures in marine and coastal areas, salt lakes, and saline-alkali land. The binary attack of chloride and sulfate ions

would more significantly intensify the deterioration of RC structures than the actions of a single factor [27-29]. Sulfate-induced damage on the matrix changes the durability properties of concrete and allows the corrosive ions, both sulfate and chloride ions, to penetrate into concrete more easily [32]. Worse still, the coexistence of sulfate ions in the chloride environment can convert the bound chloride ions to free chlorides in the competition of reaction with cement hydration products [23]. Both of these effects, combined with environmental factors [33], will further accelerate the rebar corrosion and thus reduce the durability of an RC structure.

To investigate the durability properties of concrete, numerous experimental studies have been conducted on the effect of sulfate ions on chloride transport properties in cement-based materials. These studies can be divided into three categories according to the invading way of chloride and sulfate ions into cement-based materials.

Table 1

Experimental studies of chloride transport property in cement-based materials under sulfate attack

Experiment category	Research method	The invading way of Cl^- and SO_4^{2-}
I	Pore Solution Expression	Internal mixing, internal mixing
II	Immersion	Internal mixing, external ingress
III	Cl^- Diffusion coefficient method	External ingress, internal mixing
IV	Immersion	External ingress, external ingress

For the first category, in early studies, some researchers mixed different sulfates and chlorides into cement pastes, extracted the pore solution, and then analyzed it to explore the influence of sulfates on chloride binding and pore solution chemistry

[34–36]. Ehtesham Hussain et al. [37] added sodium sulfate into chloride-bearing hydrated cement pastes and found that chloride concentration in the pore solution was significantly increased by the addition of sulfates. They attributed it to the reduction in the formation of Friedel's salt (FS) respectively. Xu [23] found that the chloride binding capacity of cement pastes was greatly influenced by the types of sulfates.

For the second category, some researchers immersed the chloride-bearing cement-paste specimens into different sulfate solutions, to investigate the properties of bound chlorides under sulfate attack. Xu et al. [38] evaluated the release of bound chlorides from pastes subjected to various sulfate attack and found that bound chlorides were partially released by sulfate attacks to form free chlorides due to the transformation of FS to ettringite. Similar results were reported by Geng et al., who also found chloride physical adsorption was not susceptible to sulfate attack, and that the effect of the induced release of bound chlorides on the stability of bound chlorides is insignificant [39].

For the third category, the test method used is to immerse cement-based materials in chloride, sulfate and their composite solutions in terms of sulfate effect on chloride ingress and binding during the life circle of RC structures. It is generally believed that the diffusivity of chloride ions in concrete is several times higher than that of sulfate ions [40,41]. Chloride diffusivity may be affected by moisture transport [42,43], other ions that coexist in the chloride environment [41,44–47] and the change of microstructure [48]. Feldman et al. [44] concluded that sulfate appeared to decrease the ingress rate of chloride ion into concrete from 12-month experimental data, while Tumidajski and Chan [45] further reported that the presence of sulfates decreased the

chloride diffusivity for OPC concrete specimens whereas the opposite behavior was found for the slag concrete ones over 60 months. Jin et al. [47] found that the effect of sulfate on chloride diffusion was related to the exposure period: sulfate reduced chloride diffusivity at early exposure period and increased the ingress of chloride at the later period. Moreover, the effect of sulfate ions on chloride binding was also extensively studied in the immersion test of cement-based materials. M. Frias et al. [49] found that the presence of sulfate partially inhibited the chloride binding and formation of FS since sulfate ions preferentially react with the calcium aluminate hydrates. De Weerdt et al. [50] discovered that sulfate ions reduce both chloride binding in C–S–H and AFm phases, as the C–S–H incorporates more sulfates instead of chlorides, and part of the AFm phases converts to ettringite. Besides the effect of sulfate ions on chloride binding, some researchers are also studied the effect of sulfates on chloride diffusivity. Cheng et al. [32] found that the coexisting sulfate ions enhanced chloride binding capacity and decreased the apparent chloride diffusion coefficient. Cao et al. [51] reported that the presence of sulfates inhibited chloride binding and increased chloride diffusion from a short-term perspective, while it inhibited the chloride diffusion in the long term.

The above review of experimental studies shows that the interaction between sulfate and chloride ions, especially the effect of sulfate on chloride transport, is very important for durability of RC structures. However, the impact of external sulfate attack on chloride binding and diffusion is still unclear and some indeed exist due to different test standards and conditions. Regarding the various coupling effects during the binary ingress, it is difficult to isolate the individual actions of different factors by

experimental testing. Furthermore, experimental studies are time-consuming and expensive, particularly for the long-term deterioration of concrete. To this end, numerical modelling can be seen as a complementary tool to probe into the mechanism of sulfate attack or chloride ingress in concrete. A recent review of the numerical assessment of ESA in concrete structures can be found in [52].

As mentioned above, when sulfate ions diffuse into cement-based materials, they react with cement hydration products, leading to dissolution and precipitation of several mineral phases in the pore solution. The response of the material, including the evolution of damage and even the propagation of cracks, will further, in turn, affect the ion transport. Hence, the essential components in the degradation of RC structures under ESA are the ionic diffusion, chemical reactions and corresponding response of hydration phases. Some numerical models available for ESA in the literature simulate ionic transport with the chemical reaction but ignore the material response and its effect on ionic transport [53–55]. Other models further incorporate the response of material on ionic transport [56–58]. The above numerical studies have formulated a solid background on mechanism of single sulfate attack and would underlie the analysis of coupling deterioration of concrete related to sulfate ions.

Compared with the numerical study of sulfate attack, the history of studies on chloride transport is longer [59,60]. The chloride ingress models are more systematic and comprehensive from various research scales [61,62], and can be divided into four groups [63]. The first group is the chloride transport model in a single phase [64,65]. The second group is the chloride transport model considering other species also in single-phase [66–68], including chloride removal/extraction from concrete [69–71].

The third group is about chloride transport in a multi-phase medium [72-74]. The fourth one is the chloride transport model in a multi-phase medium considering the transport of other ions, called the double-multi model [75–78]. In this group, the multi-phase structure can better reflect the heterogeneity of concrete, but the multi species include only sodium, potassium, and hydroxyl ions, and still need to be further extended to other ions, such as sulfate ions, considering the effect of sulfate ions on chloride binding and the effect of sulfate-induced damage on chloride diffusivity. More recently, Chen et al. [79] presented a diffusion-reaction model considering both chloride and sulfate ions, which is a great progress. However, the effect of ESA on chloride binding and diffusivity needs to be further clarified.

The presented literature survey indicates that the studies of single sulfate attack or chloride transport in concrete are relatively mature. However, very few tackle the dual attack of both sulfate and chloride ions numerically, and particularly the modelling work on the interactions between ESA and chloride penetration is still unavailable. It is of great significance to couple the two main deterioration processes to better study the long-term service performance of concrete. In this paper, a coupled model is proposed for both sulfate and chloride ions transport in concrete. A reduction function, characterizing the influence of sulfate ions on chloride binding, is proposed. A damage function was then involved in chloride diffusivity to consider the effect of sulfate-induced damage. The model is validated against third-party experimental data from multiple perspectives. And the findings could give explanations to the contradictions between the conclusions of different experiments and bring insights to the durability design of RC structures under binary sulfate and chloride attack.

2. Method

2.1. Framework and mechanism analysis

To better simulate the interaction between sulfate and chloride ions in marine concrete structures, especially the effect of sulfate ions and sulfate-induced damage on chloride binding and diffusion in concrete, two assumptions are addressed here before the modelling. Firstly, the concrete is saturated, where ionic transport is mainly controlled by the concentration gradient, namely diffusion. Secondly, the concrete is contaminated by chlorides first, equivalent to the concrete mixed with chlorides and then is exposed to ESA due to the faster ingress rate of chloride ions than sulfate ones, which agrees with the second category of the experimental studies in Section 1.

The proposed framework of the coupled model, incorporating ionic diffusion, chemical reaction, ionic binding, pore refinement as well as damage evolution, is shown in Fig. 1. This model combines two typical deterioration processes of the RC structures: external sulfate attack (ESA) and chloride transport.

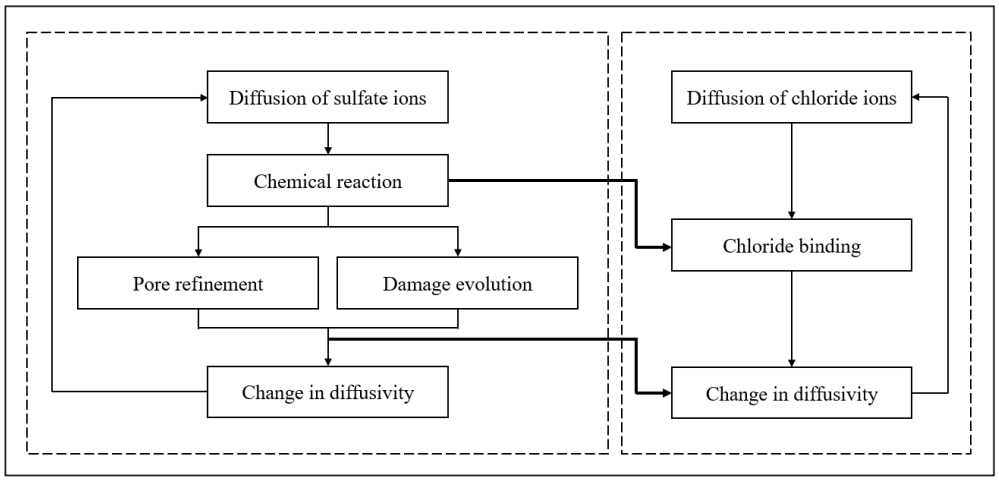

Fig. 1. Framework of the presented coupled model between (a) ESA process; (b) Chloride transport process.

By considering the mutual coupling effect of three modules, i.e., sulfate ion diffusion, chemical reaction and corresponding response of hydration phases, the process of ESA was modelled in Section 2.2.1. As for the process of the chloride transport, by modifying the mass conservation equations and nonlinear binding isotherm, the chloride diffusion model considering the binding effect was constructed in Section 2.2.2. Subsequently, the coupled model was proposed by a novel reduction function and a damage function, characterizing the sulfate influence on chloride binding and the effect of sulfate-induced damage on chloride diffusivity, respectively. The influence mechanism of sulfate ingress on chloride binding capacity and the sulfate-induced damage evolution on chloride diffusivity are illustrated in Fig. 2.

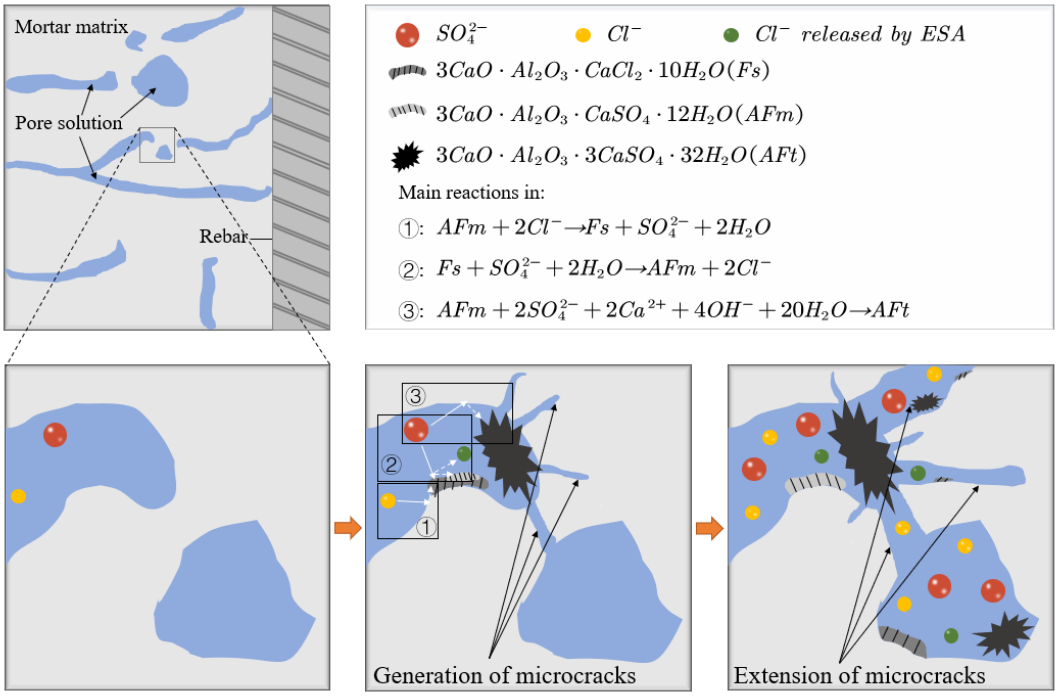

Fig. 2 Mechanisms during ion transport and material damage in concrete under binary sulfate and chloride attack.

2.2. Numerical implementation

In this section the governing equations, considering ionic diffusion and binding, chemical reaction, pore refinement as well as damage evolution, for sulfate and chloride attack in concrete are offered in Section 2.2.1 and 2.2.2 respectively. Then a novel reduction function is constructed to combine these two deterioration processes.

2.2.1 External sulfate ingress

The driving force of transport of sulfate ions in saturated concrete is mainly diffusion. According to Fick's second law and the kinetics theory of chemical reaction, the governing equation of sulfate ions can be expressed as:

$$\frac{\partial \mathrm{C}_s}{\partial t} = \frac{\partial}{\partial x}\left(D_s \frac{\partial \mathrm{C}_s}{\partial x} \right) - S_d \tag{1}$$

where C_s is the concentration of sulfate ions, t is diffusion time, x is the distance from the surface, D_s is the effective diffusion coefficient of sulfate ions in matrix. Note that mortar and ITZs are connected directly in the present model and the governing equation is adopted for them in the same form with different diffusivity. The details of ionic diffusivity in mortar and ITZs will be clarified in Section 2.3. The S_d is the dissipative source term due to a series of reaction between sulfates and cement hydrated products and was deducted from a global form (Eq. (2)) lumped by these chemical reactions [80–82], shown by Fig. 3. The term S_d can be defined by Eq. (3).

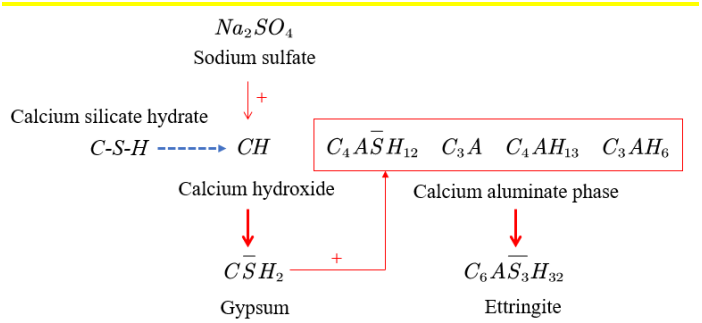

Fig. 3 Schematic diagram of the chemical reactions in concrete under sulfate attack

$$CA+q\bar{S} \rightarrow C_6A\bar{S}_3H_{32} \tag{2}$$

$$S_d = k \cdot C_s \cdot U_{CA} \tag{3}$$

where CA signifies an equivalent grouping of the reacting calcium aluminates, q represents the weighted average stoichiometric coefficient of the lumped reaction, $\bar{S}$ represents SO_3, $C_6A\bar{S}_3H_{32}$ represents ettringite, k is the reaction rate between sulfates and cement hydration products, U_{CA} is the concentration of calcium aluminates described as [83]:

$$U_{CA} = C_{CA} \cdot \left(1 - h + \frac{1}{2} \cdot C_{gyp} \cdot h + C_{gyp} \cdot h \cdot e^{-\frac{1}{6}k \cdot C_s \cdot t}\right) \cdot e^{-\frac{1}{3}k \cdot C_s \cdot t} \tag{4}$$

where C_{CA} and C_{gyp} are the initial content of calcium aluminates and gypsum, respectively. Note that Eq. (4) is also deduced from the lumped reaction form. The hydration degree h is described as [84]:

$$h = 1 - 0.5\left[\left(1+1.67\tau\right)^{-0.6} + \left(1+0.29\tau\right)^{-0.48}\right] \tag{5}$$

where τ is the hydration time. Herein, τ is related to the curing time of concrete and the immersion time of concrete in external sulfate solution, thus it can be expressed as the function of diffusion time t. Note that Eq. (5) should be modified when applied to concrete with mineral admixtures.

Due to the continuous hydration of cement and the damage caused by ESA, the effective diffusion coefficient of sulfate ions D_s can be obtained:

$$D_s = \left(\varphi_w + D_a\right) D_{s0} \tag{6}$$

where D_{s0} is the diffusion coefficient of sulfate ions in a porous medium, φ_w is the porosity of concrete which changes with the hydration process of cement, defined by Eq.(6) [85], D_a is the damage evolution caused by ESA, defined by Eq. (7) [57]. Note that by utilizing Eq. (6), the effect of pore refinement and damage evolution in concrete under sulfate attack on ionic diffusivity could be directly investigated, showed in Fig. 4.

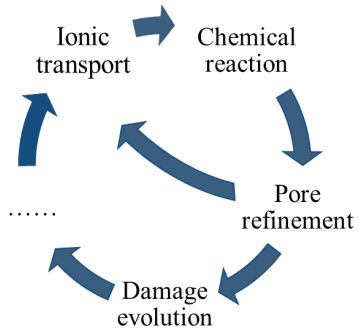

Fig. 4 Key components in concrete under sulfate attack

$$\varphi_{\mathrm{w}} = V_c \cdot \left(\frac{w}{c} - 0.39h\right) / \left(\frac{w}{c} + 0.32\right) \tag{7}$$

$$D_a = \left(1-\varphi_0\right)\left[1-\exp\left(-b_D \frac{t}{t_0}\right)\right]\left[1-\frac{1}{1+c_D\left(\frac{C_s}{C_{s0}}\right)^{d_D}}\right] \tag{8}$$

where V_c is the volume fraction of cement in concrete, w/c is the water-cement ratio, φ_0 is the initial porosity of concrete, b_D, c_D, and d_D are dimensionless empirical parameters, t_0 is a time parameter, C_{s0} is the concentration of sulfate ions in the erosion

solution. Note that Eq. (8) directly links the concentration of sulfate ions in concrete, the time of sulfate attack and the sulfate-induced damage in concrete. And by using this function, the predicted concentration distribution of sulfate ions was in good agreement with the experimental data [57].

Given the difference of geometric model between Sun's study and this study, in which concrete is considered as a 3-phase material, the governing equation should be modified as:

$$D_s = a_D\left(\varphi_w + D_a\right)D_{s0} \tag{9}$$

where a_D is an adjustment coefficient to consider the difference of aggregate grading between the model and experiment.

2.2.2 Chloride transport

Based on the mass conservation of chloride ions in a unit volume of concrete and the Fick's second law, chloride diffusion in saturated concrete can be expressed as:

$$\frac{\partial C_f}{\partial t} + \frac{\partial C_b}{\partial t} = \frac{\partial}{\partial x}\left(D_{cl}\frac{\partial C_f}{\partial x}\right) \tag{10}$$

where C_f and C_b denote the concentration of free and bound chloride ions, respectively, t is diffusion time, x is the diffusion depth, and D_{cl} is the effective diffusion coefficient of chloride ions in matrix. When sulfates are absent in the chloride environment, the diffusivity of chloride ions can be assumed as:

$$D_{cl} = a_D \cdot \varphi_w \cdot D_{cl0} \tag{11}$$

where D_{cl0} is the chloride diffusivity in the pore solution in concrete, and the parameters a_D and φ_w are the same as the ones used in Eq. (9). Since chloride ions diffuse much faster than sulfate ions [86] (e.g. Rio and Turriziani indicated the

diffusivity of chloride ions in cement was twice that of sulfate ions [87]), the chloride diffusivity in the pore solution herein is assumed as three times of that of sulfate ions.

The mass concentration of bound chloride ions can be described as:

$$\frac{\partial C_b}{\partial t} = -k_b \left(C_b - C_b^{eq} \right) \tag{12}$$

where k_b is the reaction rate between chloride ions and cement hydrated products, C_b^{eq} is the concentration of bound chloride ions when a dynamic equilibrium is reached between free and bound chloride ions. As for chloride binding, there are three categories of binding isotherm: Linear isotherm, Langmuir isotherm and Freundlich isotherm. Linear isotherm is only used for simple calculation. Chloride binding isotherm obeys Langmuir equation at low free chloride concentrations and Freundlich equation at high concentrations [17]. In this work, 0.5 mol/L NaCl solution was mixed into concrete, so the Langmuir isotherm is chosen to characterize the chloride binding capacity. Then the bound chloride concentration at dynamic equilibrium C_b^{eq} is defined as:

$$C_b^{eq} = \frac{\alpha \cdot C_f}{1 + \beta \cdot C_f} \tag{13}$$

where α and β are the binding constants of chloride, which are related to binder type. These two parameters are determined according to different test conditions. Substituting Eq. (13) into Eq. (12), it yields:

$$\frac{\partial C_b}{\partial t} = -k_b \left(C_b - \frac{\alpha \cdot C_f}{1 + \beta \cdot C_f} \right) \tag{14}$$

2.2.3 Coupling of sulfate-chloride attack

Sulfate and chloride ions coexist around the RC structures in marine and coastal

areas, salt lakes, and saline-alkali land. In such combined chloride-sulfate environment, the environmental attack on concrete structures would be more serious due to the following two main reasons. First, sulfate-induced damage on the matrix accelerates the diffusion rate of harmful ions into concrete. Second, the coexistence of sulfate ions would set some bound chloride ions free, causing the increase of free chloride ion concentration in the pore solution.

In contrast to Eq. (11), further considering the effect of sulfate-induced damage on the concrete matrix, the chloride diffusivity can be revised as:

$$D_{cl} = a_D \cdot \left(\varphi_w + D_a\right) \cdot D_{cl0} \tag{15}$$

As for the effect of sulfate attack on chloride binding, it has been long recognized that the FS will decompose in the presence of sulfate ions [39,88], which can be explained by Eq. (15). For the time being, only the chemical binding of chloride ions is considered in this work. There are three reasons: Firstly, it has been found that the physical adsorption only accounts for a very small fraction of the total bound chloride ions in Portland cement, particularly when chlorides ions transport with sulfates [89,90]. Secondly, the decomposition of FS under sodium sulfate attack is the dominant role in the release of bound chlorides [90]. Thirdly, the stability of chlorides physically absorbed by C–S–H gel is not susceptible to sodium sulfate attack [91–93].

$$3CaO{\cdot}Al_2O_3{\cdot}CaCl_2{\cdot}10H_2O\ (FS) + SO_4^{2-} + 2H_2O \rightarrow 3CaO{\cdot}Al_2O_3{\cdot}CaSO_4{\cdot}12H_2O\ (AFm) + 2Cl^- \tag{16}$$

When the concrete is under the binary corrosion of sulfates and chlorides, the bound chloride concentration at dynamic equilibrium C_b^{eq} in concrete could be

assumed as shown in Eq. (17).

$$C_b^{eq} = \left[1 - f_{re}\left(C_s\right)\right] \frac{\alpha \cdot C_f}{1 + \beta \cdot C_f} \tag{17}$$

where $f_{re}(C_s)$ is a reduction function related to the concentration of intrusion sulfate ions. The reduction function $f_{re}(C_s)$ needs to satisfy the condition of $f_{re}(0) = 0$ and $f_{re}(C_s) < 1$. Among several mathematical functions, two potential ones shown herein were further selected for trial due to their reasonable development trends:

$$f_{re}\left(C_s\right) = 1 - \frac{1}{1 + m\left(\frac{C_s}{C_{s0}}\right)^n} \tag{18}$$

$$f_{re}\left(C_s\right) = 1 - e\left(-k\frac{C_s}{C_{s0}}\right) \tag{19}$$

where m, n and k are parameters related to the speed of reduction effect, C_{s0} is the sulfate concentration in external environment of concrete. The physical meaning of these parameters will be discussed in detail in Section 4.3.

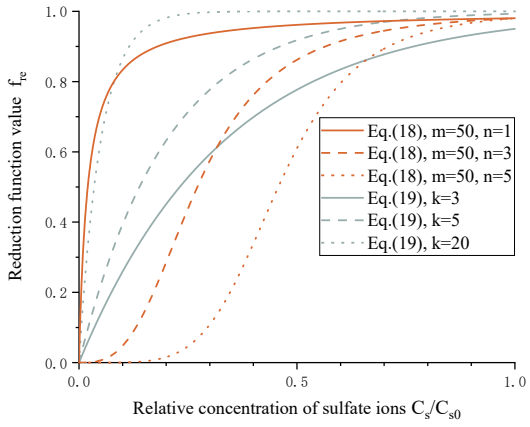

Fig. 5. Reduction functions with different forms and parameters.

Fig. 5 shows the trend of the two reduction functions. Both functions satisfy the conditions: When C_s=0, there is no sulfate attack in concrete, so the reduction

function should be 0. Under this condition, only chloride ingress occurs in concrete. When C_s=C_{s0}, there is enough sulfates to release bound chloride ions, so the reduction function should be close to 1. The chloride binding and sulfate attack are combined in concrete under this condition. But we can see further that the Eq. (18) is more in line with the law of the chemical reaction, since the effect of sulfate ions on chloride binding is little when the sulfate concentration is low. Therefore, Eq. (18) is selected as the reduction function. A detailed discussion of the reduction function, including the selection and the elaboration of the physical meaning of the parameters, will be given in section 4.3. Substituting Eq. (18) and Eq. (17) into Eq. (14), it yields:

$$\frac{\partial C_b}{\partial t} = -k_b \left[C_b + \frac{1}{1+m\left(\frac{C_s}{C_{s0}}\right)^n} \times \frac{\alpha \cdot C_f}{1+\beta \cdot C_f} \right] \tag{20}$$

By now, the whole system for the modeling of ESA and its effect on chloride binding and diffusion has been presented. The relationship between free and bound chloride ions in chloride-contaminated concrete under ESA can be elaborated. The foundation of the geometric model, as well as the initial and boundary conditions, for all the three parts of the coupled model will be discussed in the next section.

2.3. Model foundation

To better investigate the properties of ionic transport in RC structures in service, a series of multi-phase geometric models with different aggregate distribution are developed. Fig. 6a shows the three levels of the marine-exposed reinforced concrete structures: structure, component and material [94]. Fig. 6b shows that the concrete, a

heterogeneous composite material, is treated with three phases, i.e., mortar, coarse aggregates and their interfacial transition zones (ITZs). All the circular areas represent the coarse aggregates, the thin rings surrounding the aggregates (the blue part showed in Fig. 6b) are the ITZs, and the remaining part is the mortar matrix. The concrete specimen is modelled as a square plate with a side length of 50 cm. The radii of solid circles range from 1.5 mm to 10 mm and the aggregate volume fraction is assumed as 0.5. Note that the size of the concrete specimen and the radii of coarse aggregate can be easily changed to satisfy different test conditions and that the aggregates, with Fuller gradation, are randomly distributed. Regarding that the thickness of ITZs in concrete is only 20–50 μm [95], it is set as 30 μm in our research.

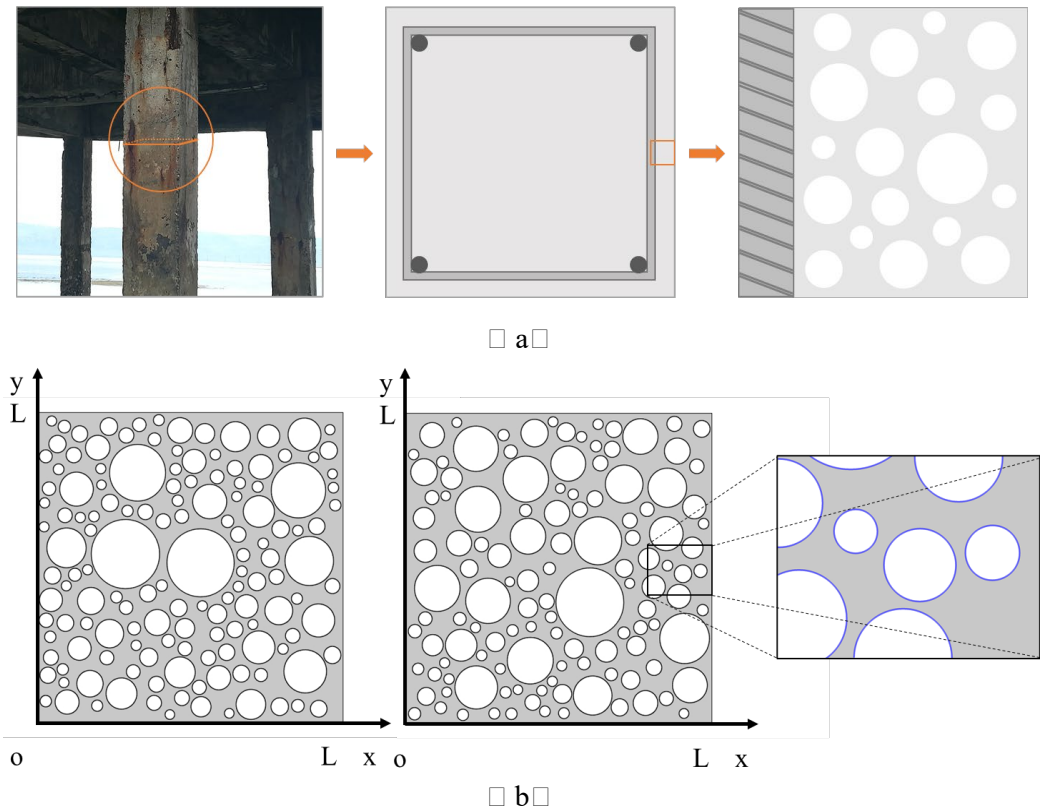

Fig. 6. Geometric modeling: (a) multi-scales of a marine-exposed reinforced concrete structure; (b) typical concrete models with ITZ and random-distributed aggregate.

It is reported in literature that aggregate shape could have influence on the ionic

penetration into concrete when ionic transport is controlled by convection, electromigration etc. or their complex coupling action [78,96]. On the other hand, the effect of aggregate shape on ionic diffusivity is very limited and could be ignored when ionic transport is under the action of simple diffusion [97–99]. Thus, concrete models with only circle coarse aggregates are used here for simplicity. Compared with the mortar matrix, aggregates are denser and have a higher resistance to the ionic diffusion, and they are therefore assumed as impermeable. Therefore, Eqs. (1), (10), (14) and (20) are only applicable to the mortar and ITZs. In other words, the diffusion of sulfate and chloride ions, the reaction between the intrusive ions and the cement hydration products and the damage evolution occur only in mortar and ITZs. Existing studies have showed that the ratio of chloride diffusivity in ITZs and mortar is about 2–15 [63,100]. Herein, the chloride and sulfate diffusivities of the ITZ are assumed to be five times of those in mortar in the present model.

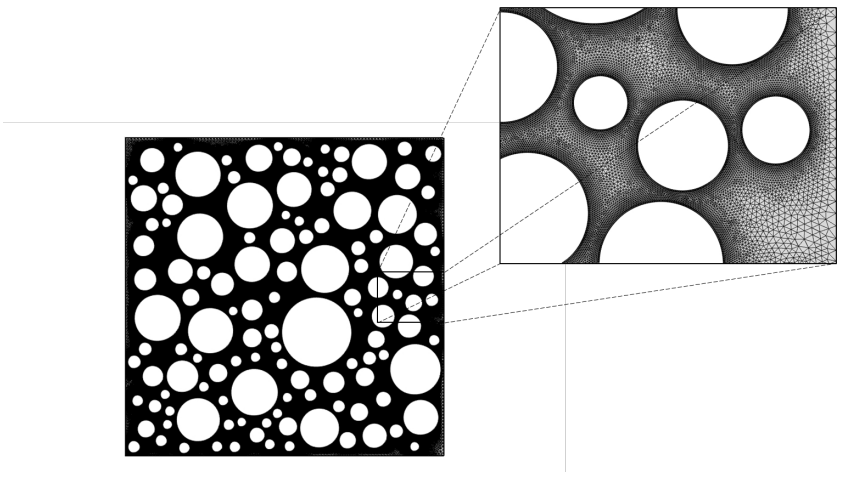

Fig. 7. Finite element meshing.

Fig. 7 shows a finite element mesh of the geometric model, from which we can see that the cement mortar and ITZs are meshed, while the aggregates are not included

because of their impermeability. Note that the accuracy of the numeral solution of Eqs. (1), (10), (14) and (20) highly depends on the size of finite element mesh. To obtain a reasonably accurate and convergent solution, the size of the finite element mesh varies between 1×10^{-6} and 5×10^{-4} m.

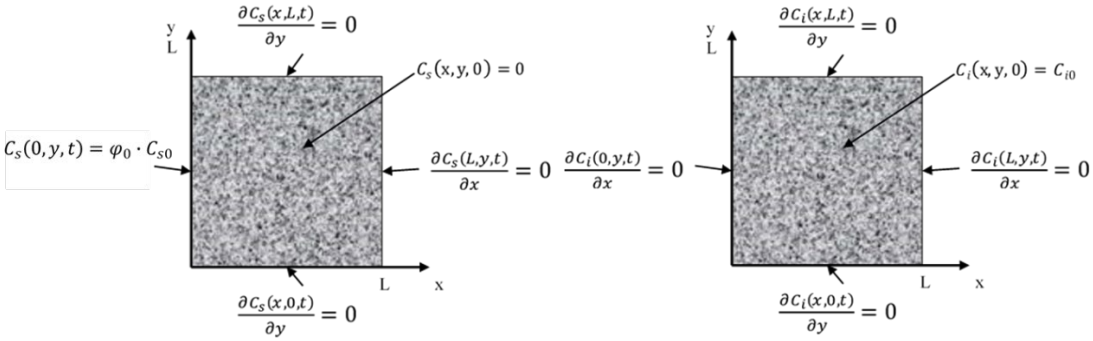

(a) External sulfate diffusion (b) Chloride binding

Fig. 8. Initial and boundary conditions for ionic transport

The initial and boundary conditions for the modeling of sulfate diffusion in 2-D concrete, i.e., the first part of the coupled model, are shown in Fig. 8a. This part is used to simulate a concrete specimen with only one side left subjected to sulfate diffusion. The left boundary of the numerical model is assumed as the Dirichlet boundary condition, and others are set as Neumann boundary conditions. Fig. 8b describes the initial and boundary conditions for the modeling of chloride ingress in chloride-bearing concrete, i.e., the second part of the coupled model. All four boundaries are set as Neumann boundary conditions. Please note that $i = f, b$ represents free and bound chloride ions respectively. C_{f0} and C_{b0} are the initial concentration of free and bound chlorides in chloride-contaminated concrete.

Combining Fig. 8a and Fig. 8b, we can get the initial and boundary conditions for the coupled model of ESA and chloride binding. The models in the present study can

be used for investigating the ionic transport properties in 2-D concrete plane due to the application of the multi-phase concrete models. The ionic transport properties in concrete, especially the interaction between changes in ionic concentration and response of individual phases during ionic penetration, will be elaborated in Section 4.

3. Model Calibration

Each part of the presented coupled model is calibrated by reproducing the ionic concentration profiles in three different types of cement-based materials from three different perspectives, i.e., a) sulfate ingress at different immersion time, b) chloride binding capacity at different curing time and c) chloride binding capacity under ESA at steady state. The first part of the coupled model is calibrated by reproducing sulfate concentration profile in OPC concrete. The second part is calibrated in chloride-contaminated specimen to investigate chloride binding capacity at different curing time. The last part, the coupled model, is calibrated in terms of chloride binding capacity with ESA at a relatively stable diffusion state.

3.1. Sulfate ingress at different immersion time

The first experiment is about the OPC concrete immersed in 5 % sodium sulfate solution for 90, 120, 150 and 180 days [57]. Herein a_D is selected as a constant 0.5. Table 2 gives the parametric values for the present sulfate diffusion model. Fig. 9 plots the sulfate diffusion profiles obtained by the present model, and for comparison the results of Sun et al.'s experiment and corresponding fitting model are added. Note that only 1-D line graph is plot here for a better contrast, although 2-D ionic profile can be easily obtained. Results of our model could fit the experimental data well in

concrete and particularly could provide a high-precision prediction from a long-term perspective (Fig. 9d), which is better than the results of Sun et al.'s fitting model.

Table 2

The parameters and their values used for ESA in concrete.

Parameter	Abbre.	Value
Diffusion coefficient of SO_4^{2-} in a porous medium	D_{s0}	6.69×10^{-9} m^2/s
Water to cement ratio	w/c	0.45
Initial porosity of concrete	φ_0	0.18
Volume fraction of cement in concrete	V_c	0.38
Reaction rate of sulfate ions in concrete	k	3.05×10^{-8} $m^3/mol/s$
Initial calcium aluminates content	C_{CA}	99.9 mol/m^3
Initial gypsum content	C_{gyp}	129.3 mol/m^3
Sulfate concentration in erosion solution	C_{S0}	376 mol/m^3
Fitting parameter of damage	b_D	1.743
Fitting parameter of damage	c_D	6.752
Fitting parameter of damage	d_D	3.819
Time parameter	t_0	730 days
Adjustment coefficient	a_D	0.5

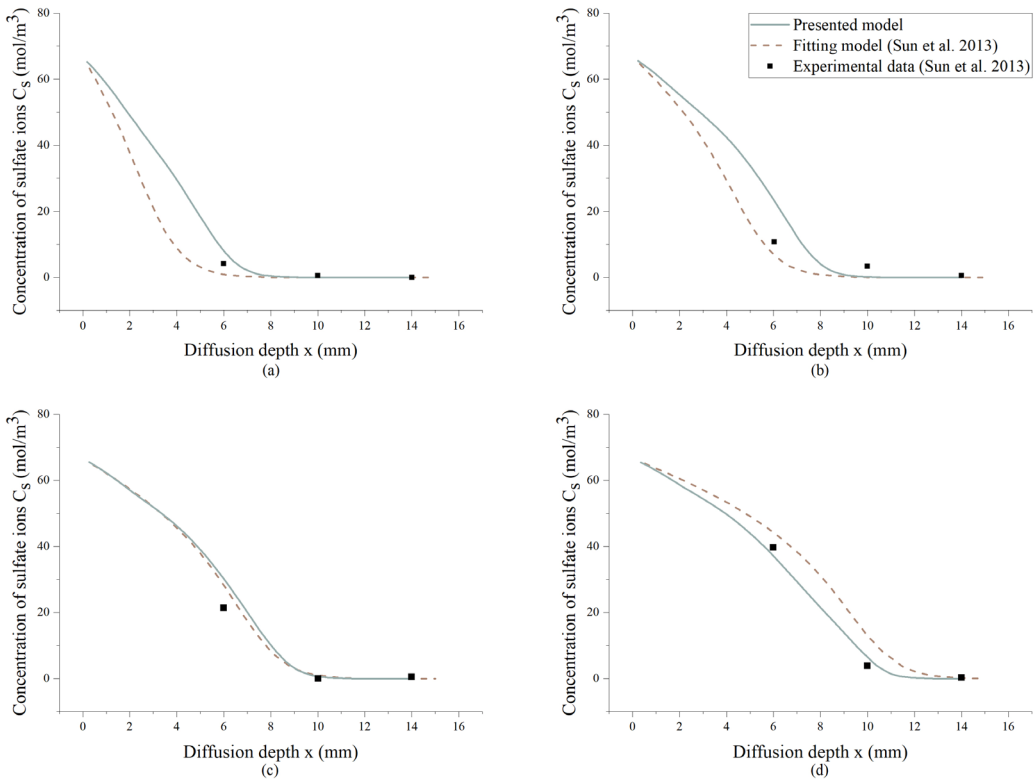

Fig. 9. Benchmark with the results of Sun et al. 's results at different immersion time: (a) 90, (b) 120, (c) 150 and (d) 180 days

3.2. Chloride binding capacity at different curing time

The second experiment used for validation is about Type 42.5 OPC mixed with 0.5 mol/L NaCl solution cured at a standard curing condition for 1,3,7,14,28,56 and 90 days [39]. Note that there is little influence to use the three-phase concrete model to reproduce the chloride profiles in OPC since aggregates effect on the ionic binding is substantially weakened due to mixing action in chloride-contaminated concrete. The dimensionless index R_{Cl} was used to characterize the concentration of bound chlorides with curing time, which is described as follows,

$$R_{cl} = \frac{C_b}{C_{t0}} \times 100\% \tag{21}$$

where C_{t0} is the initial total chloride content in cement paste. The parameters used in the present model are listed in Table 3. Note that the reaction rate for chloride binding k_b is set to 3×10^{-7}, while in some research work regarding chloride binding, the parameter k_b has been obtained by curve fitting as 3.125×10^{-7} [101] or been selected as 3.13×10^{-7} [28].

Table 3

The parameters and their values used for chloride binding.

Parameter	Abbre.	Value
Diffusion coefficient of Cl^- in a porous medium	D_{cl0}	2×10^{-8} m^2/s
Water to cement ratio	w/c	0.5
Reaction rate for chloride binding	k_b	3×10^{-7} $m^3/mol/s$
Initial free chloride concentration	C_{f0}	275 mol/m^3
Initial bound chloride concentration	C_{b0}	225 mol/m^3
Langmuir constant	α	1.65
Langmuir constant	β	0.0005 L/mol
Initial total chloride concentration	C_{t0}	500 mol/m^3

Fig. 10a. plots the obtained concentration of bound chloride ions from the present simulation at the curing time of 1,3,7,14,28,56 and 90 days. It can be seen from the bound chloride profiles that the concentration of bound chloride ions increases with the curing time. The comparison between the simulated results and experimental data is shown in Fig. 10b. The simulation results are reasonably in good agreement with the experimental data. In the early stage of curing, the R_{Cl} of the present model is slightly lower than that of experimental data. This may due to the phenomenon that there is more heat of hydration in the initial stage of cement hydration [102,103].

From Fig. 10b we can see that the value of R_{cl} eventually stabilized to about 60% with time, which means the maximum binding rate is about 60% in concrete under single chloride environment. Overall, the simulated results provide a very good tendency for the development of the concentration of bound chlorides, which indicates the present model can be used to investigate the chloride binding capacity with curing time.

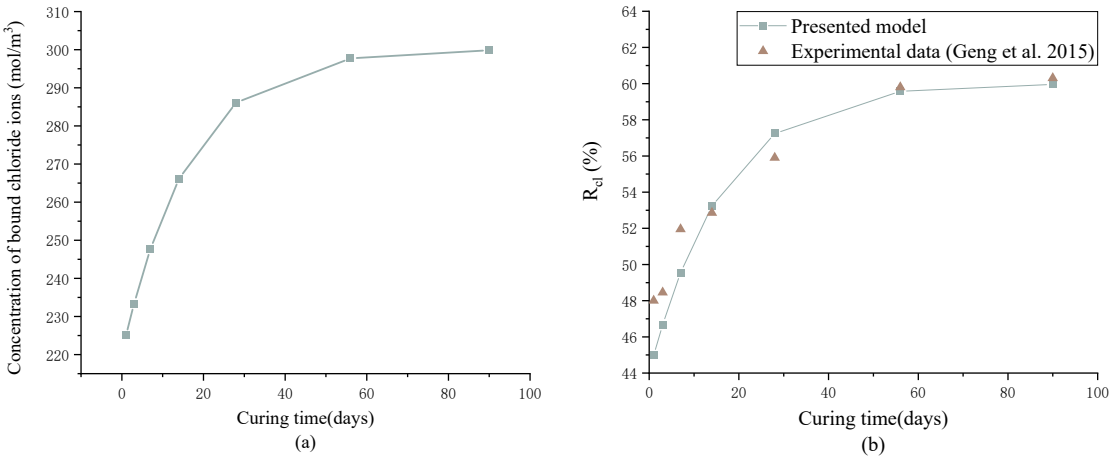

Fig. 10. Bound chlorides obtained from simulation and comparison with experimental data: (a) bound chloride profiles, and (b) R_{Cl}

3.3. **Chloride binding capacity under ESA at steady-state**

The third experiment is about No.42.5 OPC mixed with four levels of chloride ions derived from sodium chloride, ranging from 0.5% to 3% by mass of cement. After a period of 4 months curing, the demolded specimens were ground, and the specimen powder was added to 5% sodium sulfate solution [38]. The concentration of bound chloride ions was quantified until steady-state was achieved. The parameters employed in this simulation are listed in Table 4. Note that the immersion time of 3 years was determined in the simulation to achieve steady-state and the amount of cement in the mix is assumed as 426 kg/m^3. Herein, a parameter γ is used to

characterize the ratio of the concentration of bound chloride ion to that of free chloride ion in concrete after 4 months' curing, defined as,

$$\gamma=\frac{C_{b0}}{C_{f0}} \tag{22}$$

where C_{bo} and C_{f0} are the initial concentration of bound and free chloride ions.

Table 4

The parameters and their values used for the combined model.

Parameter	Abbre.	Value
Water to cement ratio	*w/c*	0.5
Binding parameter	λ	275 mol/m^3
Chloride binding capacity parameter (after 4 months' curing)	γ	0.50 (for 0.5% chlorides)
		0.50 (for 1.0% chlorides)
		0.52 (for 1.5% chlorides)
		0.55 (for 3.0% chlorides)
Langmuir constant	α	0.8
Langmuir constant	β	0.0005 L/mol

Fig. 11 shows the concentration distribution of the bound chloride after the immersion of 3-year in sodium sulfate in chloride-contaminated concrete with different levels of Na_2SO_4 solution. The distribution of bound chloride ions achieves a steady-state after 3-year immersion in Na_2SO_4 solution despite minor fluctuation. The average value of bound chloride ions is used as the stability value. Then, a comparison of bound chloride obtained in the simulation and the experiment is shown in Fig. 12. The stability values of bound chloride ions in the simulation are 0.216, 0.433, 0.623 and 1.331 (% by mass of cement), while they are 0.191, 0.437, 0.573 and

1.392 (% by mass of cement) for four different levels of total chloride, respectively. The predicted bound chlorides are in good overall agreement with the experimental data and the net concentration of bound chloride ions would continually increase with immersion time despite of the release effect of sulfate ions on chloride binding. By introducing the conception of binding rate, which is similar to Eq. (21), we can further find the binding rates in this case are 43.2%, 43.3%, 41.5% and 44.4%, respectively. Comparing the result in Section 3.2 and that in Section 3.3, it is obvious that the binding rate was off by about 18% in combined chloride-sulfate environment.

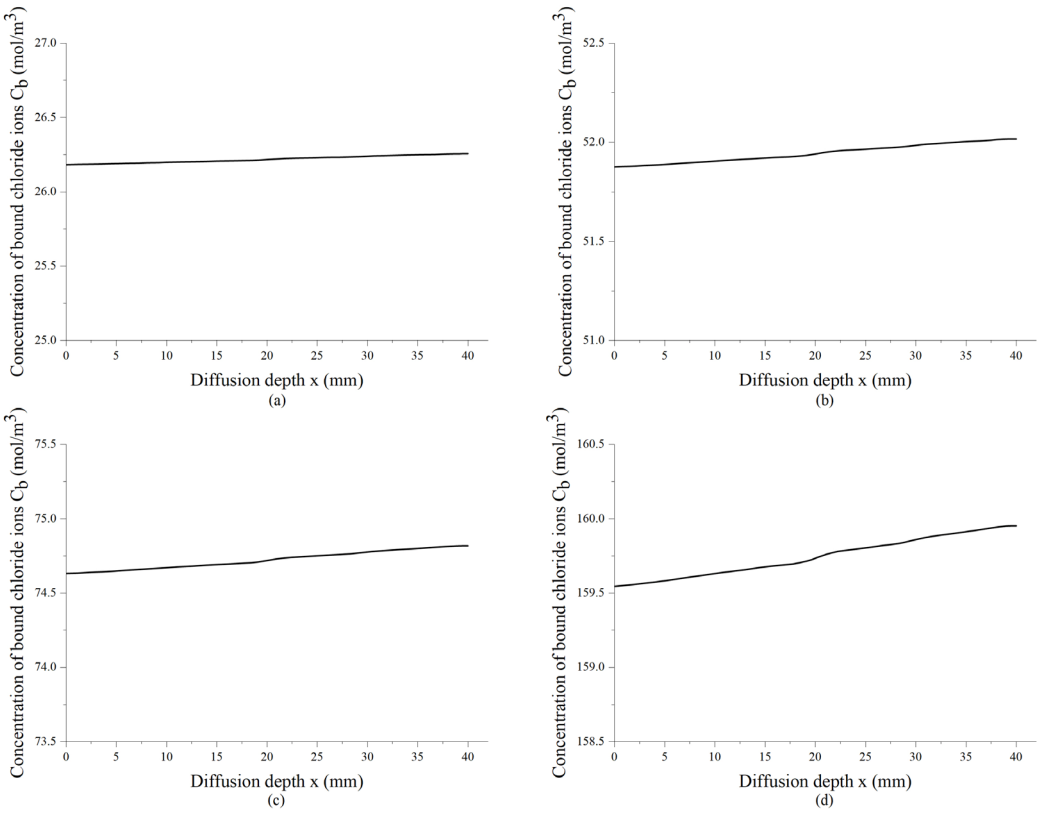

Fig. 11. Bound chloride concentration in concrete after 3-year' Na_2SO_4 attack with different levels of chlorides: (a) 0.5%, (b) 1%, (c) 1.5% and (d) 3%

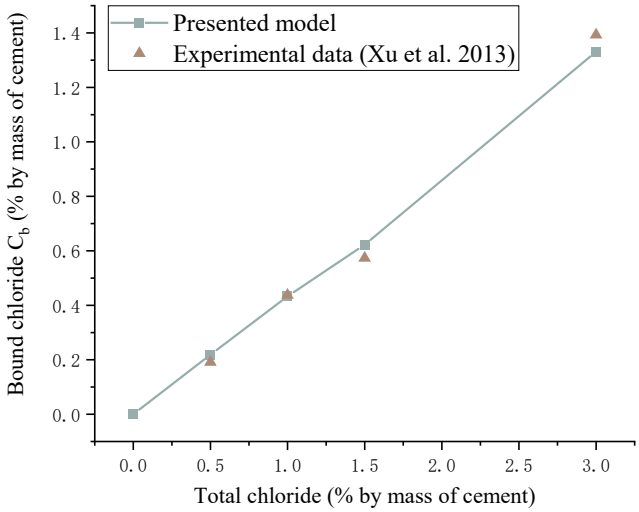

Fig. 12. Benchmark with Xu's experimental data

4. Results and Discussion

4.1. Sulfate-induced damage evolution

As is shown in Fig. 9 in Section 3.1, the ingress of sulfate ion accelerates with immersion time due to the material damage. Damage caused by sulfate diffusion accelerates ingress of harmful ions on concrete, thus affect the long-term durability of reinforced concrete structures. The line graph of the evolution of damage (defined by Eq. (7)) in concrete, mixed with 0.5 mol/L NaCl solution and immersed in 5% Na_2SO_4 solution, at the immersion time of 30, 60, 90, 120, 150 and 180 days is depicted in Fig. 13. It is apparent that the extent of damage decreases with diffusion depth, and increases with immersion time. The maximum damage value was about 0.11 at the immersion surface and gradually dropped to zero at the different diffusion depth for various immersion times. Fig. 13 also shows an interesting trend that the line graph of damage seems to be linear at an early immersion period while gradually becoming convex. Comparing Fig. 9 and Fig. 13, we can see that the ingress of sulfate

into concrete and the damage evolution are closely related.

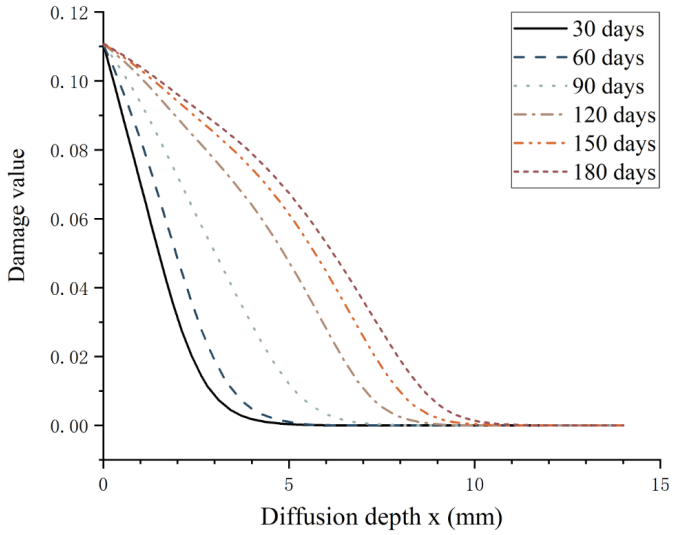

Fig. 13. Damage evolution with different immersion time

Fig. 14 shows the result of the damage in concrete, mixed with 0.5 mol/L NaCl solution and immersed in 3%, 5%, and 8% Na_2SO_4 solution, at the immersion time of 90 days. It can be seen in Fig. 14 that the higher the concentration of sulfate ions is, the higher the damage values are and the deeper the diffusion depth is.

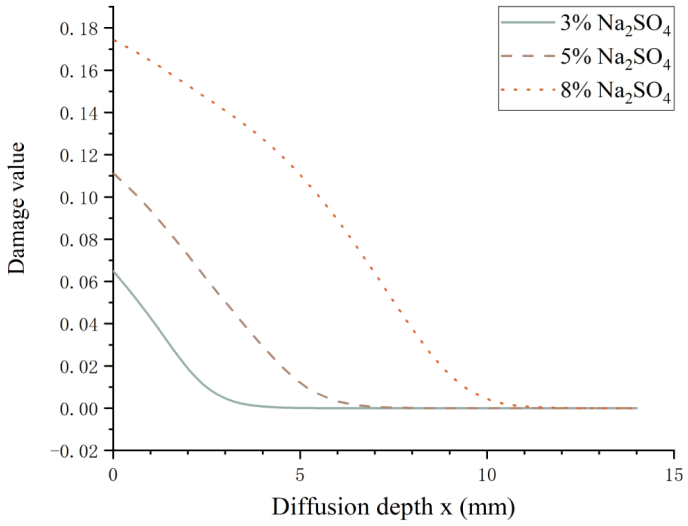

Fig. 14. Damage evolution with different concentration of Na_2SO_4 solution

Figs. 13-14 show that damage caused by sulfate attack increased with immersion time and sulfate concentration, and the damage front is linear at an early immersion period while becoming convex at the latter immersion time. When diffusing into the interior of concrete from the immersion solution, sulfates react with cement hydration products, leading to damage in concrete. With the diffusion of sulfate ions and the proceeding of the reaction, damage gradually evolves into the concrete interior. The change of the damage front from linear to convex may be due to the vicious cycle between damage and concentration of sulfate ions. Damage accelerates the diffusion of sulfate ions and thus increases the concentration of sulfate ions, and high sulfate concentration will, in turn, exacerbate the damage.

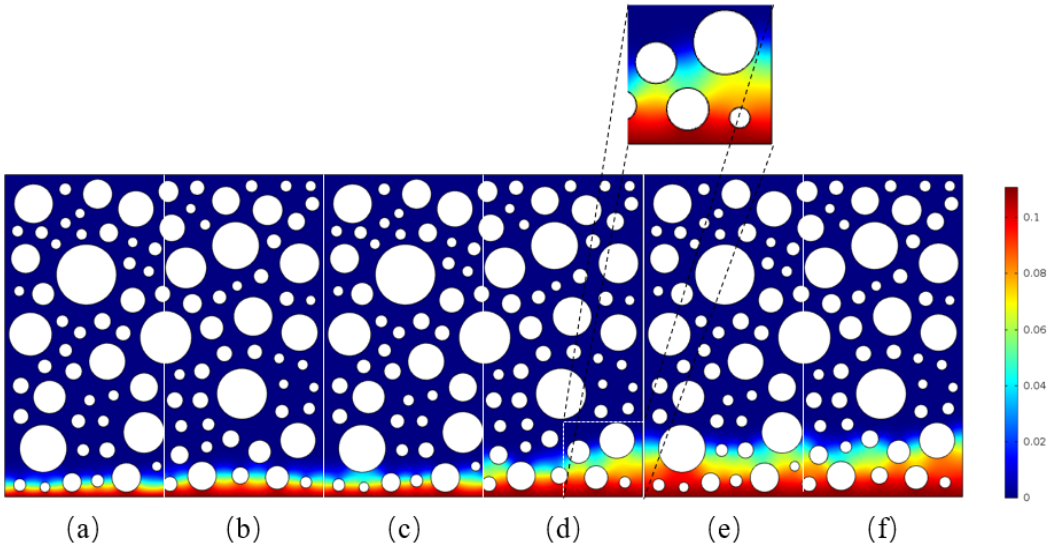

Fig. 15. Damage evolution in three-phase concrete model at the immersion time of (a) 30 days, (b) 60 days, (c) 90 days, (d) 120 days, (e) 150 days and (f) 180 days

Fig. 15 shows the damage distribution when the concrete was immersed in 5% Na_2SO_4 solution for 30, 60, 90, 120, 150 and 180 days. As we can know that there is an integral block effect of coarse aggregates on ionic transport due to the tortuosity

effect [104–106]. This indicates the presence of coarse aggregates globally mitigates the sulfate-induced damage evolution to a certain degree. Interestingly, it is important to note from Fig. 15 that the sulfate-induced damage is locally influenced by the coarse aggregate. The damage around aggregates is more serious than in the bulk mortar at the same diffusion depth, which can't be observed in the single-phase model.

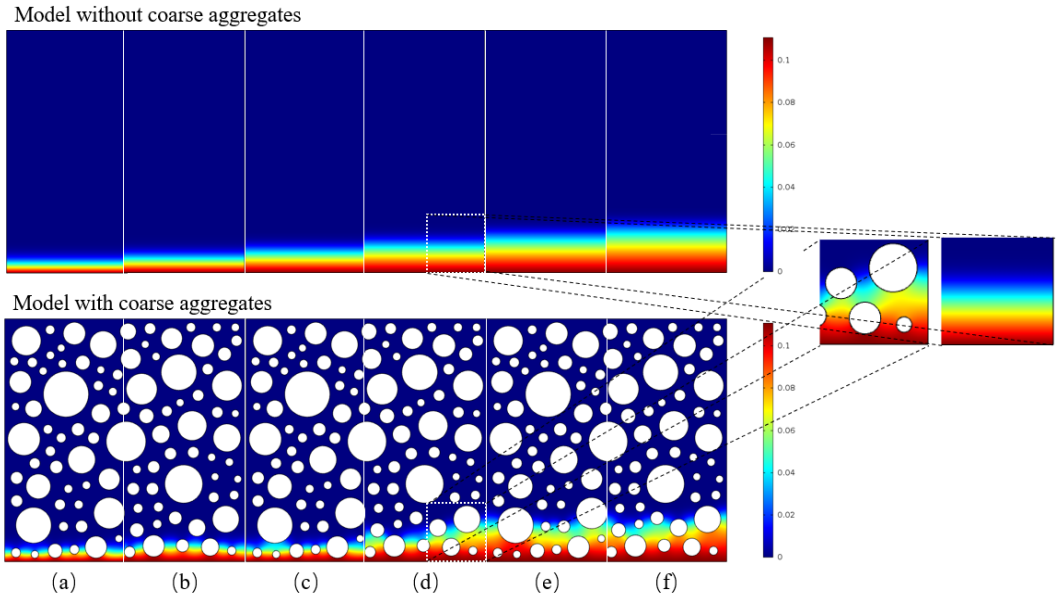

Fig. 16. Comparison of damage evolution in concrete model with and without coarse aggregates at the immersion time of (a) 30 (b) 60 (c) 90 (d) 120 (e) 150 and (f) 180 days

To further investigate the local effect of coarse aggregates on the damage evolution in concrete, a series of 2D plane pictures of the damage in concrete with and without aggregates were shown in Fig. 16. The geometric model of the concrete without aggregates is represented by a square. It is interesting to find that coarse aggregate indeed has a local effect on the sulfate-induced damage evolution, which is often ignored since it is generally believed that the presence of coarse aggregates would increase the compaction degree and improve the impermeability of concrete to

block the ionic transport. Meanwhile, we can see further that after taking the effect of coarse aggregate, including the dilute, tortuosity and ITZ effect, into consideration, the degree of damage evolution in concrete is more serious (10% ~ 30% or so) than that in concrete models without aggregates. This interesting finding that coarse aggregates locally aggravate the damage degree highlights the necessity of ionic transport in the ITZs, the weak layers between mortar paste and coarse aggregates. Existing research has found damage initiates in the ITZ [107], and the damage is more severe for concrete with higher ITZs volume content [108].

4.2. Sulfate diffusion analysis

To analyze the influence factors of sulfate diffusion so as to guide the sulfate resistance design of concrete, Fig. 17 shows the obtained sulfates concentration distribution profiles in concrete, mixed with 0.5 mol/L NaCl solution and then immersed in 5% Na_2SO_4 solution at the immersion time of 90 days, with different curing time. We can see that at the same immersion time, the longer the curing time is, the lower the concentration of sulfate ions is. The diffusion depths of sulfates are found to be 8.5, 6.8, 5.9 and 5.6 mm for the curing time of 28, 56, 90 and 120 days.

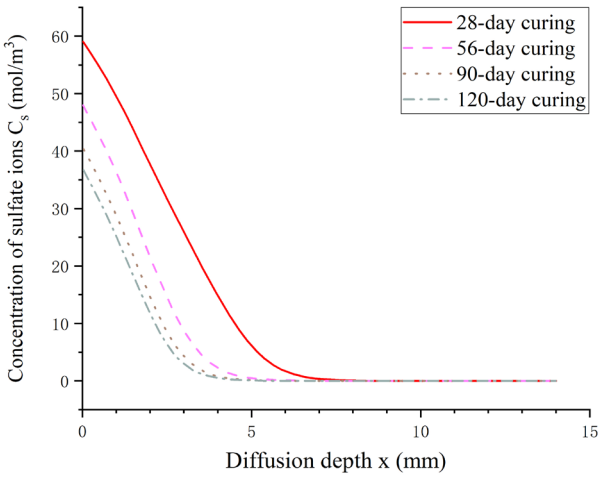

Fig. 17. Concentration distribution of sulfate ions in concrete with different curing time at the immersion time of 90 days

Fig. 18 shows the predicted sulfates concentration distribution profiles for the concrete, mixed with 0.5 mol/L NaCl solution for the curing time of 28 days and immersed in 5% Na_2SO_4 solution at the immersion time of 90 days, with different water to cement ratio. It is found that the higher the water to cement ratio is, the more penetrated sulfate ions are. The diffusion depths of sulfate ions are 6.6, 7.3, 8.2 and 8.8 mm for the w/c ratio 0.45, 0.5, 0.55 and 0.6, respectively.

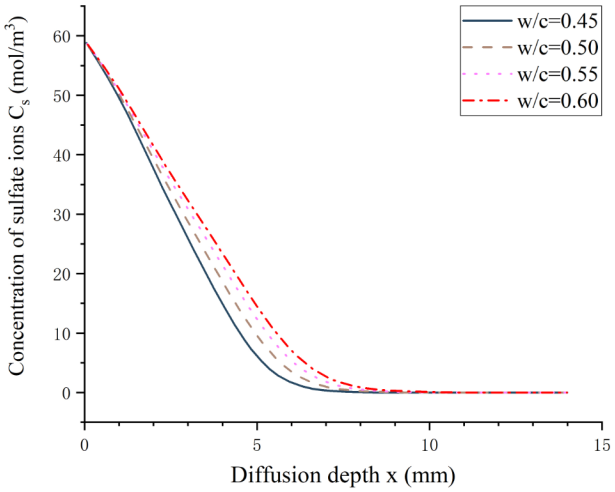

Fig. 18. Concentration distribution of sulfate ions in concrete with different water to cement ratios at the immersion time of 90 days

Additionally, we can see from the comparison of Fig. 17 and Fig. 16 that the influence region and degree of curing time and water to cement ratio on sulfates diffusion are different. Overall, the impact of curing time on sulfate diffusion is deeper than that of water to cement ratio. The water-cement ratio mainly affects ion transport in the concrete interior, while curing time also affects ion transport in the region closed to concrete surface. Compared with reducing the *w/c* ratio, increasing the curing time seems effective for improving the sulfate resistance of concrete.

4.3. Effect of sulfate ions on chloride binding

To investigate the release effect of sulfate attack on chloride binding, especially the chemical binding, a reduction function was created in the present model, which is defined as Eq. (17). From Section 3.2, we have found that the chloride binding capacity increases with the increase of curing time and eventually stabilized to about 60% (without sulfate attack). From Section 3.3, we have studied the steady-state binding capacity of chloride ions under the effect of sulfate attack by utilizing the proposed reduction function and found that the values of binding capacity range from 41.5% to 44.4%. Consequently, the chloride binding capacity declined about 18% in combined chloride-sulfate environment.

After the validity of the reduction function, the physical meaning of the parameters need to be further elucidated. The reduction function f_{re} is a function of parameters of m, n, C_s. Since f_{re} should satisfy the condition that $0 \leqslant f_{re} \leq 1$, $f_{re}(C_s=0)=0$ and $f_{re}(C_s=C_{s0})=1$, the parameter m should be any number as long as m is large enough. Fig. 19 shows the reduction function value with different parameters m and n under the different relative concentrations of sulfate ions. We can see from Fig. 19 that the impact of parameter n is larger than that of parameter m. In this study, n is defined as a release rate factor of the chloride binding effect influenced by external sulfate attack from the perspective of chemical reaction. In the rest part of this study, m is chosen as a constant 50 and n is chosen to be a constant 3. When $C_s=0$, there is no sulfate attack in concrete, so the reduction function should be 0. When $C_s=C_{s0}$, there is enough sulfates to release bound chloride ions, so the reduction function

should infinitely close to 1.

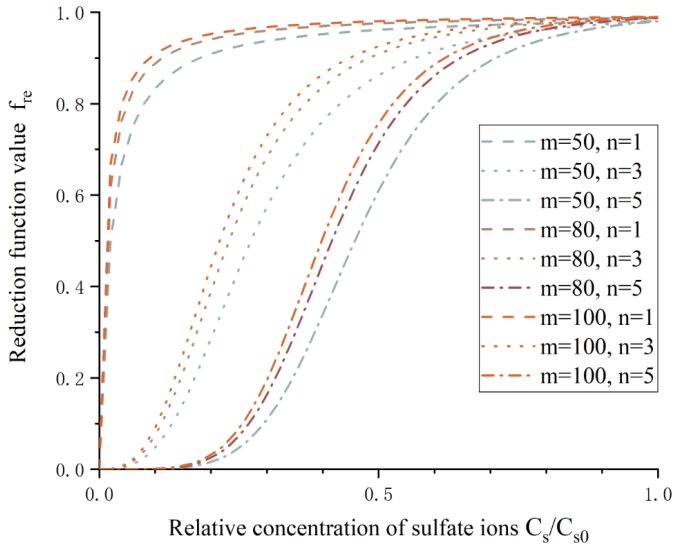

Fig. 19. Effect of different parameters m and n on reduction function values against different relative concentrations of sulfate ions.

To further investigate the effect of sulfate attack on chloride binding capacity using the proposed reduction function f_{re}, Fig. 20 shows the concentration profiles of bound chloride ions in concrete, mixed with 0.5 mol/L NaCl solution and immersed in three different levels of Na_2SO_4 solution, after 28 days' curing and 180 days' immersion. It can be easily seen from Fig. 20 that the bound chloride concentration in concrete immersed in 0% Na_2SO_4 solution is similar to that in concrete soaked in the maximum 10% Na_2SO_4 solution. This interesting finding shows that the binding mechanism of chloride ions in concrete under binary attack of chlorides and sulfates is different from that in concrete under single chloride environment. In combined chloride-sulfate environment, for one thing, the amount of chemical bound of chloride ions would decrease [23,37,38]. For another, the quantity of chloride ions adsorbed in gypsum and/or ettringite increase, although there is a slight decline in the amount of

chloride ions in calcium silicate hydrate (C-S-H) [39]. Therefore, the effect of sulfate attack on chloride binding should be considered comprehensively through the above three parts and the chloride ions adsorbed in gypsum and/or ettringite must be carefully considered.

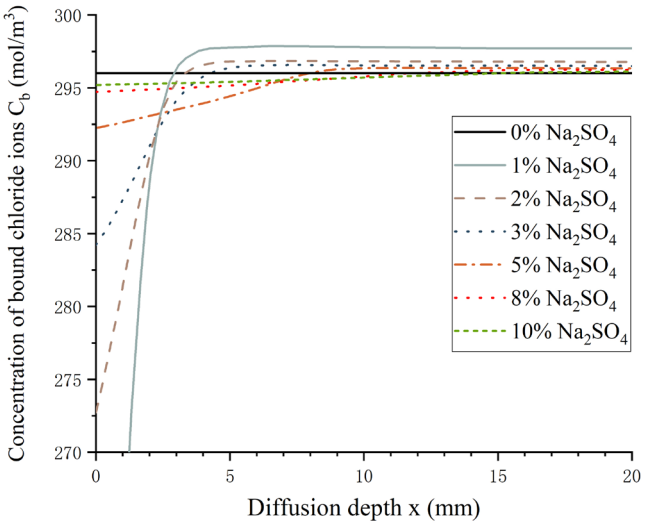

Fig. 20. Effect of Na_2SO_4 dosage on concentration distributions of bound chloride ions throughout the specimen.

We can also see from Fig. 20 that the chloride binding effect is significantly affected by the external sulfate concentration. More specifically, the region of release effect is much deeper with the higher concentration of sulfates in concrete, while the effect of sulfate ions on chloride binding became smaller with the increasing of the external sulfate concentrate, which can be explained by the following three reasons. Firstly, the release of chemically bound chloride ions is triggered when sulfate ions are coexisting with chloride ions in concrete. There are two primary chemical reactions in concrete under sulfate attack: the reaction of sulfate ions and calcium ions

to form gypsum and that of the formed gypsum with tricalcium and dicalcium aluminate. However, due to the initial reaction between chlorides and calcium aluminates to form Friedel's salts (FS), i.e., the chloride chemical binding, the effect of subsequent sulfate attack is that the chloride ions in FS are replaced by the sulfate ions, thus the chemically bound chloride ions in FS are released. Secondly, apart from the release of the chemically bound chloride ions caused by sulfate attack, the amount of physically adsorbed chloride ions in C-S-H also decreases. But the products of the reaction between sulfate and cement clinker could adsorb more chloride ions physically. The concentration of sulfate ions in the simulation is much larger than that in actual seawater. A higher concentration of sulfate ions will produce more gypsum in concrete, which improves the physical adsorption of chloride ions to some extent. Thirdly, the corrosion products are mainly gypsum in concrete at high sulfate concentration [109]. Compared with ettringite formed at relatively low sulfate concentration, the volume expansion of concrete caused by gypsum is much lower [109], which slows down the rate of corrosion and chemical binding of chloride ions. Further, the second finding indicates that the degree of release effect of sulfates on bound chloride increase with the higher relative concentration of sulfate ions (C_s / C_{s0}), which proves the viability of the reduction function (Eq. (17)) established by the form of the relative concentration of sulfate ions in concrete.

4.4. Effect of sulfate-induced damage on chloride diffusivity

As mentioned in Section 4.1, material damage greatly accelerates the ingress of harmful ions into concrete, so the evolution of sulfate-induced damage would

definitely facilitate the chloride diffusion. Fig. 21 shows the change of the relative effective diffusivity of chloride ions in concrete, mixed with 0.5 mol/L NaCl solution for 28 days' curing and immersed in 5% Na_2SO_4 solution, at the long-term immersion of 3, 6, 9, 12, 18 and 24 months. Note that the chloride diffusivity at the immersion time of 0 month is set as initial diffusivity and the relative chloride diffusivity at the other immersion time is defined as the ratio of the chloride diffusivity at a given immersion time to the initial diffusivity.

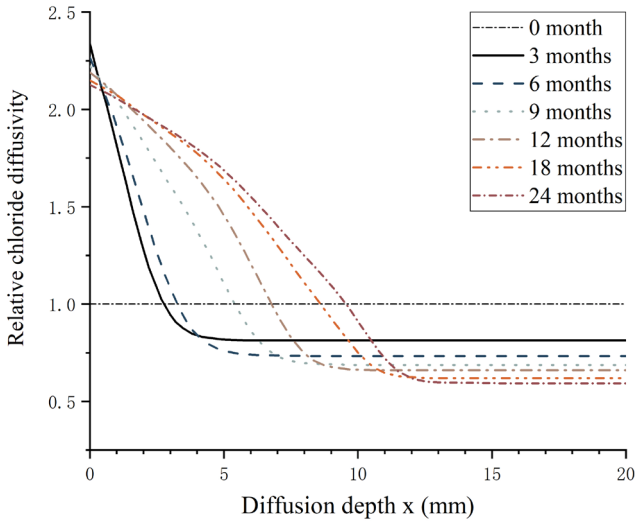

Fig. 21. Effect of damage and pore-refinement on relative chloride diffusivity.

It is indicated in Fig. 21 that each diffusivity line can be divided into two parts. One is a curve segment, and the other is a horizontal line segment. The change of the curve segment was mainly caused by the damage and the maximum chloride diffusivity became about 2.5 times as much as the initial diffusivity due to the sulfate-induced damage. Moreover, the trend of the curve segment remains consistent with the damage evolution. The change of the horizontal line segment was caused by

the pore-refinement effect in concrete. And the values of horizontal lines decrease with the immersion time. The relative chloride diffusivities are 0.813, 0.732, 0.687, 0.660, 0.620 and 0.593 at the immersion time of 3, 6, 9, 12, 18 and 24 months, respectively, which indicates that the chloride diffusivity in concrete decreases with the immersion time because of the pore-refinement during the cement hydration.

Corresponding to the two parts of effective chloride diffusivity in concrete shown in Fig. 21, the degradation of chloride-contaminated concrete due to sulfate attack can be divided into two zones: damaged zone and non-damaged zone. In the damaged zone, the diffusivity of chloride ions increases with time due to two main reasons. One is that the damage caused by sulfate attack will increase the connectivity of pores in concrete, which greatly broadens the channel of ionic transport. The other is that the chloride ions in FS are replaced by the sulfate ions, thus the chemically bound chloride ions in FS are released to form free ones. Under higher concentration gradient, chloride ions in concrete diffuse much faster. In the non-damaged zone, there is almost no effect of sulfates on the diffusion of chloride ions. The continued decrease of the chloride diffusivity with time is mainly caused by the pore-refinement in concrete. The chloride diffusivity in the damaged zone is 5~10 times that in the non-damaged zone, which shows that both the sulfate-induced damage, the release effect of sulfate attack on chloride binding and the pore-refinement can significantly influence the chloride diffusivity.

5. Conclusions

Reinforced concrete (RC) structures would suffer from serious durability

problems caused by chloride ingress and sulfate attack during long-term service. To investigate the ionic transport and influence mechanism in concrete under the dual attacks of chlorides and sulfates, this study presents a coupled model for sulfate attack and its effect on chloride binding and diffusion. From the presented numerical investigation, the following conclusions can be drawn:

a) There is a vicious cycle between damage evolution and sulfate ingress in concrete. The damage front is linear in an early immersion stage while becoming convex in the latter immersion stage, which means the deterioration of concrete under sulfate attack is more and more serious with service time.
b) Due to the ITZ effect, the presence of course aggregates locally aggravates the evolution of sulfate-induced damage by 10% ~ 30%.
c) Both the curing time and the water-cement ratio of concrete affect sulfate transport. Compared with reducing the water-cement ratio, increasing the curing time can do better in improving the sulfate resistance of concrete.
d) A reduction function was proposed for the release effect of sulfate attack on chloride binding. It is proved that the chloride binding capacity declined about 18% in combined chloride-sulfate environment by using this reduction function.
e) The degradation process of chloride-contaminated concrete due to ESA can be divided into two zones: damaged zone and non-damaged zone. Not only the damaged zone but also the non-damaged zone influences the chloride

diffusivity. The chloride diffusivity in the former increases with the sulfate-induced damage evolution and the higher concentration gradient, while in the latter it decreases with the pore-refining process. The chloride diffusivity in the damaged zone is 5~10 times that in the non-damaged zone.

The above findings may bring insights to the durability design of RC structures under coupled sulfate and chloride attack. However, the present work is limited to saturated concrete and neglects the effect of electric field interaction between heterogeneous ions for the time being. For further research studies, the model could be improved considering multi-ions effect and applied to unsaturated condition.

Acknowledgements

This work was funded by the National Natural Science Foundation of China [51978396] and the Shanghai Rising-Star Program, China [19QA1404700]. The authors also would like to thank the supports from the Young Elite Scientists Sponsorship Program by CAST [2018QNRC001], the State Key Laboratory of High Performance Civil Engineering Materials [2018CEM006] and the State Key Laboratory of Structural Analysis for Industrial Equipment [GZ18119].

References

[1] O. Al-Amoudi, Attack on plain and blended cements exposed to aggressive sulfate environments, Cem. Concr. Compos. 24 (2002) 305–316. https://doi.org/10.1016/S0958-9465(01)00082-8.

[2] A. Neville, The confused world of sulfate attack on concrete, Cem. Concr. Res. 34 (2004) 1275–1296. https://doi.org/10.1016/j.cemconres.2004.04.004.

[3] M.F. Lei, L.M. Peng, C.H. Shi, S.Y. Wang, Experimental study on the damage mechanism of tunnel structure suffering from sulfate attack, Tunn. Undergr. Sp. Technol. 36 (2013) 5–13. https://doi.org/10.1016/j.tust.2013.01.007.

[4] Z.Q. Liu, F.Y. Zhang, D.H. Deng, Y.J. Xie, G.C. Long, X.G. Tang, Physical sulfate attack on concrete lining–A field case analysis, Case Stud. Constr. Mater. 6 (2017) 206–212. https://doi.org/10.1016/j.cscm.2017.04.002.

[5] P.W. Brown, S. Badger, Distributions of bound sulfates and chlorides in concrete subjected to mixed NaCl, MgSO4, Na2SO4 attack, Cem. Concr. Res. 30 (2000) 1535–1542. https://doi.org/10.1016/S0008-8846(00)00386-0.

[6] J.K. Chen, M.Q. Jiang, Long-term evolution of delayed ettringite and gypsum in Portland cement mortars under sulfate erosion, Constr. Build. Mater. 23 (2009) 812–816. https://doi.org/10.1016/j.conbuildmat.2008.03.002.

[7] A. Bonakdar, B. Mobasher, Multi-parameter study of external sulfate attack in blended cement materials, Constr. Build. Mater. 24 (2010) 61–70. https://doi.org/10.1016/j.conbuildmat.2009.08.009.

[8] A.J. Al-Tayyib, S.K. Somuah, J.K. Boah, P. Leblanc, A.I. Al-Mana, Laboratory study on the effect of sulfate ions on rebar corrosion, Cem. Concr. Res. 18 (1988) 774–782. https://doi.org/10.1016/0008-8846(88)90102-0.

[9] A.J. Al-Tayyib, M. Shamim Khan, Effect of sulfate ions on the corrosion of rebars embedded in concrete, Cem. Concr. Compos. 13 (1991) 123–127. https://doi.org/10.1016/0958-9465(91)90007-5.

[10] Q. Liu, Z. Hu, X. Lu, J. Yang, I. Azim, W. Sun, Prediction of chloride distribution for offshore concrete based on statistical analysis, Materials (Basel). 13 (2020) 174.

[11] Q. Liu, M.F. Iqbal, J. Yang, X. Lu, P. Zhang, M. Rauf, Prediction of chloride diffusivity in concrete using artificial neural network: Modelling and performance evaluation, Constr. Build. Mater. (2020) 121082.

[12] M.F. Iqbal, Q. Liu, I. Azim, X. Zhu, J. Yang, M.F. Javed, M. Rauf, Prediction of mechanical properties of green concrete incorporating waste foundry sand based on gene expression programming, J. Hazard. Mater. 384 (2020) 121322.

[13] Y. Ma, Z. Guo, L. Wang, J. Zhang, Experimental investigation of corrosion effect on bond behavior between reinforcing bar and concrete, Constr. Build. Mater. 152 (2017) 240–249.

[14] B. Šavija, J. Pacheco, E. Schlangen, Lattice modeling of chloride diffusion in sound and cracked concrete, Cem. Concr. Compos. 42 (2013) 30–40. https://doi.org/10.1016/j.cemconcomp.2013.05.003.

[15] Q.F. Liu, J. Yang, J. Xia, D. Easterbrook, L.Y. Li, X.Y. Lu, A numerical study on chloride migration in cracked concrete using multi-component ionic transport models, Comput. Mater. Sci. 99 (2015) 396–416. https://doi.org/10.1016/j.commatsci.2015.01.013.

[16] Y. Ma, Z. Guo, L. Wang, J. Zhang, Probabilistic life prediction for reinforced concrete structures subjected to seasonal corrosion-fatigue damage, J. Struct. Eng. 146 (2020) 4020117.

[17] L.P. Tang, L.O. Nilsson, Chloride binding capacity and binding isotherms of OPC pastes and mortars, Cem. Concr. Res. 23 (1993) 247–253.

https://doi.org/10.1016/0008-8846(93)90089-R.
[18] T.U. Mohammed, H. Hamada, Relationship between free chloride and total chloride contents in concrete, Cem. Concr. Res. 33 (2003) 1487–1490. https://doi.org/10.1016/S0008-8846(03)00065-6.
[19] Q. Yuan, C.J. Shi, G. De Schutter, K. Audenaert, D.H. Deng, Chloride binding of cement-based materials subjected to external chloride environment - A review, Constr. Build. Mater. 23 (2009) 1–13. https://doi.org/10.1016/j.conbuildmat.2008.02.004.
[20] D.W. Li, L.Y. Li, X.F. Wang, Chloride diffusion model for concrete in marine environment with considering binding effect, Mar. Struct. 66 (2019) 44–51. https://doi.org/10.1016/j.marstruc.2019.03.004.
[21] L. Bertolini, F. Bolzoni, M. Gastaldi, T. Pastore, P. Pedeferri, E. Redaelli, Effects of cathodic prevention on the chloride threshold for steel corrosion in concrete, Electrochim. Acta. 54 (2009) 1452–1463. https://doi.org/10.1016/j.electacta.2008.09.033.
[22] C. Arya, N.R. Buenfeld, J.B. Newman, Factors influencing chloride-binding in concrete, Cem. Concr. Res. 20 (1990) 291–300. https://doi.org/10.1016/0008-8846(90)90083-A.
[23] Y. Xu, The influence of sulphates on chloride binding and pore solution chemistry, Cem. Concr. Res. 27 (1997) 1841–1850. https://doi.org/10.1016/S0008-8846(97)00196-8.
[24] G.K. Glass, N.R. Buenfeld, The influence of chloride binding on the chloride induced corrosion risk in reinforced concrete, Corros. Sci. 42 (2000) 329–344. https://doi.org/10.1016/S0010-938X(99)00083-9.
[25] J. Geng, D. Easterbrook, Q.F. Liu, L.Y. Li, Effect of carbonation on release of bound chlorides in chloride-contaminated concrete, Mag. Concr. Res. 68 (2016) 353–363. https://doi.org/doi:10.1680/jmacr.15.00234.
[26] D. Trejo, M. Shakouri, N.P. Vaddey, O.B. Isgor, Development of empirical models for chloride binding in cementitious systems containing admixed chlorides, Constr. Build. Mater. 189 (2018) 157–169. https://doi.org/10.1016/j.conbuildmat.2018.08.197.
[27] W.Q. Jiang, X.H. Shen, S.X. Hong, Z.Y. Wu, Q.F. Liu, Binding capacity and diffusivity of concrete subjected to freeze-thaw and chloride attack: A numerical study, Ocean Eng. 186 (2019) 106093. https://doi.org/10.1016/j.oceaneng.2019.05.075.
[28] X.H. Shen, W.Q. Jiang, D.S. Hou, Z. Hu, J. Yang, Q.F. Liu, Numerical study of carbonation and its effect on chloride binding in concrete, Cem. Concr. Compos. 104 (2019) 103402. https://doi.org/10.1016/j.cemconcomp.2019.103402.
[29] Omar Saeed Baghabra Al-Amoudi, M. Maslehuddin, The effect of chloride and sulfate ions on reinforcement corrosion, Cem. Concr. Res. 23 (1993) 139–146. https://doi.org/10.1016/0008-8846(93)90144-X.
[30] M. Maes, N. De Belie, Resistance of concrete and mortar against combined attack of chloride and sodium sulphate, Cem. Concr. Compos. 53 (2014) 59–72. https://doi.org/10.1016/j.cemconcomp.2014.06.013.
[31] C.L. Zhang, Q.F. Liu, Coupling Erosion of Chlorides and Sulfates in Reinforced Concrete– A Review, Mater. Rep. (2021).
[32] S.K. Cheng, Z.H. Shui, T. Sun, X. Gao, C. Guo, Effects of sulfate and magnesium ion

on the chloride transportation behavior and binding capacity of Portland cement mortar, Constr. Build. Mater. 204 (2019) 265–275. https://doi.org/10.1016/j.conbuildmat.2019.01.132.

[33] J. Mao, H. Wang, D. Feng, T. Tao, W. Zheng, Investigation of dynamic properties of long-span cable-stayed bridges based on one-year monitoring data under normal operating condition, Struct. Control Heal. Monit. 25 (2018) e2146.

[34] W.R. Holden, C.L. Page, N.R. Short, The influence of chlorides and sulphates on durability, Corros. Reinf. Concr. Constr. (1983) 143–150.

[35] H.A.F. Dehwah, M. Maslehuddin, S.A. Austin, Effect of sulfate ions and associated cation type on the pore solution chemistry in chloride-contaminated plain and blended cements, Cem. Concr. Compos. 25 (2003) 513–525. https://doi.org/10.1016/S0958-9465(02)00091-4.

[36] M. Maslehuddin, P.C. Rasheeduzzafar, A. Al-Mana, A. Al-Tayyib, Effect of temperature and sulfate contamination on the chloride binding capacity of cements, in: Proc. 4th Int. Conf. Deterior. Repair Reinf. Concr. Arab. Gulf,(GL Macmillan, 1993: pp. 735--750.

[37] S. Ehtesham Hussain, Rasheeduzzafar, A.S. Al-Gahtani, Influence of sulfates on chloride binding in cements, Cem. Concr. Res. 24 (1994) 8–24. https://doi.org/10.1016/0008-8846(94)90078-7.

[38] J.X. Xu, C.K. Zhang, L.H. Jiang, L. Tang, G.F. Gao, Y.P. Xu, Releases of bound chlorides from chloride-admixed plain and blended cement pastes subjected to sulfate attacks, Constr. Build. Mater. 45 (2013) 53–59. https://doi.org/10.1016/j.conbuildmat.2013.03.068.

[39] J. Geng, D. Easterbrook, L.Y. Li, L.W. Mo, The stability of bound chlorides in cement paste with sulfate attack, Cem. Concr. Res. 68 (2015) 211–222. https://doi.org/10.1016/j.cemconres.2014.11.010.

[40] Oberholster, RE, Pore structure, permeability and diffusivity of hardened cement paste and concrete in relation to durability: status and prospects, in: 8th Int. Congr. Chem. Cem., 1986: pp. 323--335.

[41] R.F. Bakker, Permeability of blended cement concretes, Spec. Publ. 79 (1983) 589--606.

[42] M.Z. Zhang, G. Ye, K. Van Breugel, Modeling of ionic diffusivity in non-saturated cement-based materials using lattice Boltzmann method, Cem. Concr. Res. 42 (2012) 1524–1533. https://doi.org/10.1016/j.cemconres.2012.08.005.

[43] A. Caggiano, D. Said Schicchi, C. Mankel, N. Ukrainczyk, E.A.B. Koenders, A mesoscale approach for modeling capillary water absorption and transport phenomena in cementitious materials, Comput. Struct. 200 (2018) 1–10. https://doi.org/10.1016/j.compstruc.2018.01.013.

[44] R. Feldman, J. Beaudoio, K. Philipose, Effect of cement blends on chloride and sulfate ion diffusion in concrete, II Cem. 88 (1991) 3--18.

[45] P.J. Tumidajski, G.W. Chan, Effect of sulfate and carbon dioxide on chloride diffusivity, Cem. Concr. Res. 26 (1996) 551–556. https://doi.org/10.1016/0008-8846(96)00019-1.

[46] H.A.F. Dehwah, M. Maslehuddin, S.A. Austin, Long-term effect of sulfate ions and

associated cation type on chloride-induced reinforcement corrosion in Portland cement concretes, Cem. Concr. Compos. 24 (2002) 17–25. https://doi.org/10.1016/S0958-9465(01)00023-3.

[47] Z.Q. Jin, W. Sun, Y.S. Zhang, J.Y. Jiang, J.Z. Lai, Interaction between sulfate and chloride solution attack of concretes with and without fly ash, Cem. Concr. Res. 37 (2007) 1223–1232. https://doi.org/10.1016/j.cemconres.2007.02.016.

[48] N. Ukrainczyk, E.A.B. Koenders, Representative elementary volumes for 3D modeling of mass transport in cementitious materials, Model. Simul. Mater. Sci. Eng. 22 (2014). https://doi.org/10.1088/0965-0393/22/3/035001.

[49] M. Frias, S. Goñi, R. García, R.V. De La Villa, Seawater effect on durability of ternary cements. Synergy of chloride and sulphate ions, Compos. Part B Eng. 46 (2013) 173–178. https://doi.org/10.1016/j.compositesb.2012.09.089.

[50] K. De Weerdt, D. Orsáková, M.R. Geiker, The impact of sulphate and magnesium on chloride binding in Portland cement paste, Cem. Concr. Res. 65 (2014) 30–40. https://doi.org/10.1016/j.cemconres.2014.07.007.

[51] Y.Z. Cao, L.P. Guo, B. Chen, Influence of sulfate on the chloride diffusion mechanism in mortar, Constr. Build. Mater. 197 (2019) 398–405. https://doi.org/10.1016/j.conbuildmat.2018.11.238.

[52] T. Ikumi, I. Segura, Numerical assessment of external sulfate attack in concrete structures. A review, Cem. Concr. Res. 121 (2019) 91–105. https://doi.org/10.1016/j.cemconres.2019.04.010.

[53] P.N. Gospodinov, R.F. Kazandjiev, T.A. Partalin, M.K. Mironova, Diffusion of sulfate ions into cement stone regarding simultaneous chemical reactions and resulting effects, Cem. Concr. Res. 29 (1999) 1591–1596. https://doi.org/10.1016/S0008-8846(99)00138-6.

[54] F. Schmidt-Döhl, F.S. Rostásy, Model for the calculation of combined chemical reactions and transport processes and its application to the corrosion of mineral-building materials: Part I. Simulation model, Cem. Concr. Res. 29 (1999) 1039–1045. https://doi.org/10.1016/S0008-8846(99)00087-3.

[55] E. Samson, J. Marchand, Modeling the transport of ions in unsaturated cement-based materials, Comput. Struct. 85 (2007) 1740–1756. https://doi.org/10.1016/j.compstruc.2007.04.008.

[56] S. Sarkar, S. Mahadevan, J.C.L. Meeussen, H. van der Sloot, D.S. Kosson, Numerical simulation of cementitious materials degradation under external sulfate attack, Cem. Concr. Compos. 32 (2010) 241–252. https://doi.org/10.1016/j.cemconcomp.2009.12.005.

[57] C. Sun, J.K. Chen, J. Zhu, M.H. Zhang, J. Ye, A new diffusion model of sulfate ions in concrete, Constr. Build. Mater. 39 (2013) 39–45. https://doi.org/10.1016/j.conbuildmat.2012.05.022.

[58] S.S. Qin, D.J. Zou, T.J. Liu, A. Jivkov, A chemo-transport-damage model for concrete under external sulfate attack, Cem. Concr. Res. 132 (2020). https://doi.org/10.1016/j.cemconres.2020.106048.

[59] W.Q. Jiang, Q.F. Liu. Chloride Transport in Concrete Subjected to Freeze-Thaw Cycles – A Short Review. J Chin Ceram Soc, 2020, 48(2): 258–272.

[60] M.F. Iqbal, M.F. Javed, M. Rauf, I. Azim, M. Ashraf, J. Yang, Q.F. Liu. Sustainable utilization of foundry waste: Forecasting mechanical properties of foundry sand based concrete using multi-expression programming. Science of the Total Environment (2021).

[61] D. Hou, W. Zhang, M. Sun, P. Wang, M. Wang, J. Zhang, Z. Li, Modified Lucas-Washburn function of capillary transport in the calcium silicate hydrate gel pore: A coarse-grained molecular dynamics study, Cem. Concr. Res. 136 (2020) 106166.

[62] K. Zhao, Y. Qiao, P. Zhang, J. Bao, Y. Tian, Experimental and numerical study on chloride transport in cement mortar during drying process, Constr. Build. Mater. 258 (2020) 119655.

[63] Q.F. Liu, D. Easterbrook, J. Yang, L.Y. Li, A three-phase, multi-component ionic transport model for simulation of chloride penetration in concrete, Eng. Struct. 86 (2015) 122–133. https://doi.org/10.1016/j.engstruct.2014.12.043.

[64] R.K. Dhir, M.R. Jones, S.L.D. Ng, Prediction of total chloride content profile and concentration/time-dependent diffusion coefficients for concrete, Mag. Concr. Res. 50 (1998) 37–48. https://doi.org/10.1680/macr.1998.50.1.37.

[65] T. Maheswaran, J.G. Sanjayan, A semi-closed-form solution for chloride diffusion in concrete with time-varying parameters, Mag. Concr. Res. 56 (2004) 359–366. https://doi.org/10.1680/macr.2004.56.6.359.

[66] O. Truc, J.P. Ollivier, L.O. Nilsson, Numerical simulation of multi-species transport through saturated concrete during a migration test - MsDiff code, Cem. Concr. Res. 30 (2000) 1581–1592. https://doi.org/10.1016/S0008-8846(00)00305-7.

[67] B. Johannesson, K. Yamada, L.O. Nilsson, Y. Hosokawa, Multi-species ionic diffusion in concrete with account to interaction between ions in the pore solution and the cement hydrates, Mater. Struct. Constr. 40 (2007) 651–665. https://doi.org/10.1617/s11527-006-9176-y.

[68] B.B. Guo, Y. Hong, G.F. Qiao, J.P. Ou, A COMSOL-PHREEQC interface for modeling the multi-species transport of saturated cement-based materials, Constr. Build. Mater. 187 (2018) 839–853. https://doi.org/10.1016/j.conbuildmat.2018.07.242.

[69] L.Y. Li, C.L. Page, Modelling of electrochemical chloride extraction from concrete: Influence of ionic activity coefficients, Comput. Mater. Sci. 9 (1998) 303–308. https://doi.org/10.1016/s0927-0256(97)00152-3.

[70] L.Y. Li, C.L. Page, Finite element modelling of chloride removal from concrete by an electrochemical method, Corros. Sci. 42 (2000) 2145–2165. https://doi.org/10.1016/S0010-938X(00)00044-5.

[71] Y. Wang, L.Y. Li, C.L. Page, A two-dimensional model of electrochemical chloride removal from concrete, Comput. Mater. Sci. 20 (2001) 196–212. https://doi.org/10.1016/S0927-0256(00)00177-4.

[72] S. Caré, E. Hervé, Application of a n-phase model to the diffusion coefficient of chloride in mortar, Transp. Porous Media. 56 (2004) 119–135. https://doi.org/10.1023/B:TIPM.0000021730.34756.40.

[73] Z. Hu, L.X. Mao, J. Xia, J. Bin Liu, J. Gao, J. Yang, Q.F. Liu, Five-phase modelling for effective diffusion coefficient of chlorides in recycled concrete, Mag. Concr. Res. 70 (2018) 593–594. https://doi.org/10.1680/jmacr.17.00194.

[74] L. Mao, Z. Hu, J. Xia, G. Feng, I. Azim, J. Yang, Q. Liu, Multi-phase modelling of electrochemical rehabilitation for ASR and chloride affected concrete composites, Compos. Struct. 207 (2019) 176–189.

[75] Q.F. Liu. Multi-phase modelling of concrete at meso-micro scale based on multi-species transport. J Chin Ceram Soc, 2018, 46(08): 1074-1080.

[76] Q.F. Liu, J. Xia, D. Easterbrook, J. Yang, L.Y. Li, Three-phase modelling of electrochemical chloride removal from corroded steel-reinforced concrete, Constr. Build. Mater. 70 (2014) 410–427. https://doi.org/10.1016/j.conbuildmat.2014.08.003.

[77] G.L. Feng, L.Y. Li, B. Kim, Q.F. Liu, Multiphase modelling of ionic transport in cementitious materials with surface charges, Comput. Mater. Sci. 111 (2016) 339–349. https://doi.org/10.1016/j.commatsci.2015.09.060.

[78] Q.F. Liu, G.F. Feng, J. Xia, J. Yang, L.Y. Li, Ionic transport features in concrete composites containing various shaped aggregates: a numerical study, Compos. Struct. 183 (2018) 371–380. https://doi.org/10.1016/j.compstruct.2017.03.088.

[79] Z. Chen, L.Y. Wu, V. Bindiganavile, C.F. Yi, Coupled models to describe the combined diffusion-reaction behaviour of chloride and sulphate ions in cement-based systems, Constr. Build. Mater. 243 (2020) 118232. https://doi.org/10.1016/j.conbuildmat.2020.118232.

[80] X.B. Zuo, W. Sun, C. Yu, Numerical investigation on expansive volume strain in concrete subjected to sulfate attack, Constr. Build. Mater. 36 (2012) 404–410. https://doi.org/10.1016/j.conbuildmat.2012.05.020.

[81] R. Tixier, B. Mobasher, Modeling of Damage in Cement-Based Materials Subjected to External Sulfate Attack. I: Formulation, J. Mater. Civ. Eng. 15 (2003) 305–313. https://doi.org/10.1061/(ASCE)0899-1561(2003)15:4(305).

[82] A.E. Idiart, C.M. López, I. Carol, Chemo-mechanical analysis of concrete cracking and degradation due to external sulfate attack: A meso-scale model, Cem. Concr. Compos. 33 (2011) 411–423. https://doi.org/10.1016/j.cemconcomp.2010.12.001.

[83] X.B. Zuo, W. Sun, Full process analysis of damage and failure of concrete subjected to external sulfate attack, J Chin Ceram Soc. 37 (2009) 1063–1067. https://doi.org/10.14062/j.issn.0454-5648.2009.07.027.

[84] M. Masi, D. Colella, G. Radaelli, L. Bertolini, Simulation of chloride penetration in cement-based materials, Cem. Concr. Res. 27 (1997) 1591–1601.

[85] H. Song, J.K. Chen, Effect of damage evolution on poisson's ratio of concrete under sulfate attack, Acta Mech. Solida Sin. 24 (2011) 209–215. https://doi.org/10.1016/S0894-9166(11)60022-0.

[86] R. Bakker, Permeability of blended cement concretes, Spec. Publ. 79 (1983) 589–606.

[87] A. Rio, R. Turriziani, No Title, Cem. 80 (1983) 37–48.

[88] J.O. Ukpata, P.A.M. Basheer, L. Black, Slag hydration and chloride binding in slag cements exposed to a combined chloride-sulphate solution, Constr. Build. Mater. 195 (2019) 238–248. https://doi.org/10.1016/j.conbuildmat.2018.11.055.

[89] P. Henocq, J. Marchand, E. Samson, J.-A. Lavoie, Modeling of ionic interactions at the C–S–H surface—Application to CsCl and LiCl solutions in comparison with NaCl solutions, in: 2nd Int. Symp. Adv. Concr. through Sci. Eng. RILEM Proc., RILEM Publications France, 2006.

[90] J. Geng, D. Easterbrook, L.Y. Li, L.W. Mo, The stability of bound chlorides in cement paste with sulfate attack, Cem. Concr. Res. 68 (2015) 211–222. https://doi.org/10.1016/j.cemconres.2014.11.010.

[91] P. Henocq, Modeling ionic interactions on the surface of calcium silicate hydrates, French. PhD Thesis. Laval Univ. (2005).

[92] C. Zhang, Z. Ge, K. Yang, Q. Wei, Adsorption Characteristic of Calcium Silicate Hydrate Surface for SO~ 4^ 2^-Ions, J Chin Ceram Soc. 33 (2005) 926.

[93] Y. Elakneswaran, T. Nawa, K. Kurumisawa, Electrokinetic potential of hydrated cement in relation to adsorption of chlorides, Cem. Concr. Res. 39 (2009) 340–344.

[94] C. Wu, C. Chen, C. Cheeseman. Size effects on the mechanical properties of 3D printed plaster and PLA parts. J Mater Civil Eng. DOI: 10.1061/(ASCE)MT.1943-5533.0003787

[95] S. Diamond, J. Huang, The ITZ in concrete - A different view based on image analysis and SEM observations, Cem. Concr. Compos. 23 (2001) 179–188. https://doi.org/10.1016/S0958-9465(00)00065-2.

[96] S. Dehghanpoor Abyaneh, H.S. Wong, N.R. Buenfeld, Computational investigation of capillary absorption in concrete using a three-dimensional mesoscale approach, Comput. Mater. Sci. 87 (2014) 54–64. https://doi.org/10.1016/j.commatsci.2014.01.058.

[97] L.Y. Li, J. Xia, S.S. Lin, A multi-phase model for predicting the effective diffusion coefficient of chlorides in concrete, Constr. Build. Mater. 26 (2012) 295–301. https://doi.org/10.1016/j.conbuildmat.2011.06.024.

[98] J.J. Zheng, X.Z. Zhou, Y.F. Wu, X.Y. Jin, A numerical method for the chloride diffusivity in concrete with aggregate shape effect, Constr. Build. Mater. 31 (2012) 151–156. https://doi.org/10.1016/j.conbuildmat.2011.12.061.

[99] Q.F. Liu, D. Easterbrook, L.Y. Li, D.W. Li, Prediction of chloride diffusion coefficients using multi-phase models, Mag. Concr. Res. 69 (2017) 134–144. https://doi.org/10.1680/jmacr.16.00134.

[100] J.J. Zheng, X.Z. Zhou, Prediction of the chloride diffusion coefficient of concrete, Mater. Struct. Constr. 40 (2007) 693–701. https://doi.org/10.1617/s11527-006-9182-0.

[101] J. Geng, D. Easterbrook, Q.F. Liu, L.Y. Li, Effect of carbonation on release of bound chlorides in chloride-contaminated concrete, Mag. Concr. Res. 68 (2016) 353–363. https://doi.org/10.1680/jmacr.15.00234.

[102] D. Wang, Q. Wang, Z. Huang, New insights into the early reaction of NaOH-activated slag in the presence of CaSO4, Compos. Part B Eng. 198 (2020) 108207.

[103] S. Zhuang, Q. Wang, Inhibition mechanisms of steel slag on the early-age hydration of cement, Cem. Concr. Res. 140 (n.d.) 106283.

[104] D.W. Hobbs, Aggregate influence on chloride ion diffusion into concrete, Cem. Concr. Res. 29 (1999) 1995–1998. https://doi.org/10.1016/S0008-8846(99)00188-X.

[105] C.C. Yang, J.K. Su, Approximate migration coefficient of interfacial transition zone and the effect of aggregate content on the migration coefficient of mortar, Cem. Concr. Res. 32 (2002) 1559–1565. https://doi.org/10.1016/S0008-8846(02)00832-3.

[106] S. Caré, Influence of aggregates on chloride diffusion coefficient into mortar, Cem. Concr. Res. 33 (2003) 1021–1028. https://doi.org/10.1016/S0008-8846(03)00009-7.

[107] Z.Q. Liu, G. De Schutter, D.H. Deng, Z.W. Yu, Micro-analysis of the role of interfacial transition zone in “salt weathering” on concrete, Constr. Build. Mater. 24 (2010) 2052–2059. https://doi.org/10.1016/j.conbuildmat.2010.04.053.

[108] K. Wu, W. Kang, L.L. Xu, D.D. Sun, F.Z. Wang, G. De Schutter, Damage evolution of blended cement concrete under sodium sulfate attack in relation to ITZ volume content, Constr. Build. Mater. 190 (2018) 452–465. https://doi.org/10.1016/j.conbuildmat.2018.09.013.

[109] Z.Y. Zhang, X.G. Jin, W. Luo, Long-term behaviors of concrete under low-concentration sulfate attack subjected to natural variation of environmental climate conditions, Cem. Concr. Res. 116 (2019) 217–230. https://doi.org/10.1016/j.cemconres.2018.11.017.